Mon. Not. R. Astron. Soc. **000**, 000–000 (0000) Printed 28 December 2013 (MN LaTeX style file v1.4)

A search for hidden white dwarfs in the ROSAT EUV survey II: Discovery of a distant DA+F6/7V binary system in a direction of low density neutral hydrogen

M. R. Burleigh[1] and M. A. Barstow[1] and J. B. Holberg[2]
[1] *Department of Physics and Astronomy, University of Leicester, University Rd., Leicester, LE1 7RH*
[2] *Lunar and Planetary Laboratory, Gould-Simpson Building, University of Arizona, Tucson AZ 85721, USA*

May 27th 1998

ABSTRACT

The ROSAT Wide Field Camera (WFC) survey of the Extreme Ultraviolet (EUV) has provided us with evidence for the existence of a previously unidentified sample of hot white dwarfs in unresolved, detached binary systems. These stars are invisible at optical wavelengths due to the close proximity of their much more luminous companions (spectral type K or earlier). However, for companions of spectral type ∼A5 or later the white dwarfs are easily visible at far-ultraviolet (far-UV) wavelengths, and can be identified in spectra taken by IUE. Sixteen such systems have been discovered in this way through ROSAT, EUVE and IUE observations, including four identified by us in Paper I (Burleigh, Barstow and Fleming 1997). In this paper we report the results of our continuing search during the final year of IUE operations. One new system, RE J0500−364 (DA+F6/7V), has been identified. This star appears to lie at a distance of between ∼500−1000pc, making it one of the most distant white dwarfs, if not the most distant, to be detected in the EUV surveys. The very low line-of-sight neutral hydrogen volume density to this object could place a lower limit on the length of the β CMa interstellar tunnel of diffuse gas, which stretches away from the Local Bubble in a similar direction to RE J0500−364.

In this paper we also analyse a number of the stars observed where no white dwarf companion was found. Some of these objects show evidence for chromospheric and coronal activity. Finally, we present an analysis of the previously known WD+active F6V binary HD27483 (Böhm-Vitense 1993), and show that, at T≈22,000K, the white dwarf may be contributing significantly to the observed EUV flux. If so, it is one of the coolest such stars to be detected in the EUV surveys.

Key words: Stars: binaries – Stars: white dwarfs – X-ray: stars – Ultra-violet: stars – ISM: general.

1 INTRODUCTION

The vast majority of the >2000 known white dwarfs (McCook and Sion 1998) are isolated stars discovered at optical wavelengths by virtue of their photometric colours or proper motions. In either case, there is a strong bias against detecting any white dwarfs in unresolved binary systems. A companion star of type K or earlier will completely dominate the optical spectrum of the white dwarf, effectively rendering it invisible. Indeed, Sirius B, the first white dwarf to be discovered, would never have been resolved from the A1 dwarf Sirius were it not for the close proximity of the system to Earth (2.64pc).

Prior to the ROSAT and Extreme Ultraviolet Explorer (EUVE) surveys, a small number of unresolved white dwarf/main sequence binaries had been discovered serendiptously. For example, the white dwarf in the V471 Tauri system was found as a result of an eclipse by its active K2V companion. In addition, a number of white dwarfs have been accidently discovered during various far-ultraviolet (far-UV) observations of the normal stellar companions by the International Ultraviolet Explorer (IUE), e.g. ζ Cap (Böhm-Vitense 1980), 56 Peg (Schindler et al. 1982) and 4 σ^1 Ori (Johnson and Ake 1986), although Shipman and Geczi (1989) systematically studied the then existing IUE archive for white dwarf companions to G, K and M stars, and found no further examples.

Now, however, the extreme ultraviolet (EUV) surveys of the ROSAT Wide Field Camera (WFC, Pounds et al. 1993, Pye et al. 1995) and EUVE (Bowyer et al. 1994, 1996) have provided evidence for the existence of a substantial sample of these previously unknown white dwarfs, through the detection of EUV radiation. Sixteen new systems have been discovered in this way, including β Crateris (A2IV+WD, Fleming et al. 1991), KW Aur C (F4V+DA, Hodgkin et al. 1993), HD18131 (K0IV+DA, Vennes et al. 1995), RE J0357+283 (K2V+DA Jeffries, Burleigh and Robb 1996), and the latest two, RE J0702+129 (K0Ve+DA, Vennes et al. 1997), and HR2875 (B5V+WD, Vennes, Berghoefer and Christian 1997, Burleigh and Barstow 1998). Detailed studies of groups of these objects have been undertaken by Barstow et al. (1994) and Burleigh, Barstow and Fleming (1997, paper I). Positive identifications have been made in each case through follow-up observations in the far-UV with IUE, since for companions later than ~A5 the hot white dwarf is easily visible at these wavelengths (the companion to the B5V star HR2875 was identified through an EUVE spectrum, since the B star still dominates the spectrum at far-UV wavelengths).

It is well established that over half of all stars are members of binary or multiple systems, yet the overwhelming majority of catalogued white dwarfs are isolated objects. The new population of optically hidden white dwarfs emerging from the EUV surveys has profound implications, therefore, for our knowledge of the white dwarf luminosity function, space density and formation rate (e.g. Fleming, Liebert and Green 1986). Observations of white dwarfs in detached binary systems also allow us to place constraints on their evolutionary models (e.g. de Kool and Ritter 1993).

In this paper we report the results of a continuing search for more of these binaries in the ROSAT WFC catalogue, during the final year of IUE operations. We have discovered one new unresolved white dwarf+main sequence star binary (RE J0500−362)⋆. In the cases where no white dwarf was detected, a number of the target stars show evidence for chromospheric activity. We also present an analysis of the previously known white dwarf+active star system HD27483 (Böhm-Vitense 1993). We show that the white dwarf is contributing to the EUV flux and should be included in the growing list of EUV-emitting optically-hidden hot white dwarfs in binary systems.

2 DETECTION OF THE SOURCES IN THE ROSAT WFC EUV SURVEY

The ROSAT WFC EUV all-sky survey was conducted between July 1990 and January 1991. Two broad band filters were utilised (designated S1 and S2), and most of the count rates quoted in this paper (see Table 1) are taken from the 2RE catalogue (Pye et al. 1995). This revised list contains 479 EUV sources, as compared with 383 in the original Bright Source Catalogue (Pounds et al. 1993). The 2RE catalogue was compiled from the original survey data with improved methods for source detection, background screening etc. The resulting count rates are equivalent to on-axis, at-launch values.

The ROSAT PSPC X-ray survey was conducted simultaneously with the WFC. The soft (0.1−0.4keV) and hard (0.4-2.4keV) band count rates (Table 1) were obtained via the World Wide Web from the on-line All-Sky Survey Bright Source Catalogue, maintained by the Max-Planck Institute in Germany (Voges et al. 1996). All of the X-ray flux from hot white dwarfs is expected to lie within the soft band.

The EUVE all-sky survey was conducted in four pass bands between July 1992 and January 1993. These count rates are also given in Table 1, and are mainly taken from the Second EUVE Source Catalog (Bowyer et al. 1996) which, like the ROSAT WFC 2RE catalogue, includes better source detection algorithms and improved reliability.

2.1 Selection of candidate hidden white dwarfs

Hot white dwarfs in unresolved binaries with companions of spectral type K or earlier are virtually impossible to discern from optical spectra alone. However, it is possible to unambiguously identify these hidden white dwarfs in far-UV spectra taken by IUE. The problem is how to select likely candidates from just their EUV and soft X-ray count rates.

Most of the hot white dwarfs discovered by ROSAT have very soft spectra compared to normal stars, particularly where the interstellar hydrogen column density is low. The ratio of the WFC S2 to S1 count rates can often exceed a factor of two. Additionally, no photons are usually detected from a white dwarf above the 0.28keV carbon edge of the ROSAT PSPC. All other X-ray and EUV-emitting astronomical objects generally have spectra extending to higher energies. Thus, many of the stars originally selected for observation by IUE were relatively bright EUV sources with very similar colours to known hot white dwarfs (e.g. KW Aur C, Hodgkin et al. 1993). The success rates of the early searches by, for example, Barstow et al. (1994) were very high, and appeared to represent the tip of an iceberg.

However, many of the white dwarfs in the ROSAT WFC survey are relatively faint EUV sources, indistinguishable by count rate ratios alone from coronally active objects. Further selection criteria, in addition to simple EUV colour and brightness, needed to be applied. In Paper I (Burleigh, Barstow and Fleming 1997) we conducted a search for fainter, less obvious examples of these binary systems, with a ~40% success rate. Candidates were selected, in particular, from normal stars that had been observed in the WFC optical identification programme (Mason et al. 1995), and where little or no evidence of activity had been found. In some cases, e.g. HD2133 (RE J0024−741), a hidden white dwarf was indeed detected in an IUE SWP spectrum. In others, e.g. HR2468 (RE J0637−613), the IUE observations revealed evidence of chromospheric and coronal emission that had eluded the optical identification team.

In this paper we report the results of a further search for hidden white dwarfs during the last year of IUE operations (1995/96). Thirteen candidates were selected and observed, including many that were detected for the first time in the reprocessed ROSAT WFC 2RE data. These are, in general, faint EUV sources. In most cases, the target stars were not

⋆ Originally reported, with a preliminary analysis, in the proceedings of the 1996 European White Dwarf Workshop by Burleigh and Barstow (1997).

known to be active, and had S2/S1 count rate ratios >2. In a separate optical programme, a number of the unidentified 2RE fields were observed to try to determine the counterpart to the EUV source. In some cases, e.g. RE J0500−364, 2RE J0222+503 and 2RE J0232−025, only one relatively faint star (V>10) was visible in the field. Although a few EUV sources (mainly red dwarfs) are active stars with V>10 (e.g. Proxima Cen, M5Ve, V=11.1), most are much brighter than this. Thus, for these sources, a hidden hot white dwarf companion was a feasible explanation for the EUV radiation, and they were added to the IUE target list.

2.2 UV spectroscopy

A log of all the far-UV observations is given in Table 2. The white dwarf companion to HD27483 was serendipitously discovered in October 1992 by Böhm-Vitense (1993), independently of the ROSAT survey, during an IUE survey of Hyades F stars. RE J0500−364 was first observed in a short half-hour exposure in November 1995 (SWP56217), and a faint white dwarf was detected. A follow up spectrum, with an 8 hour exposure to achieve the required signal-to-noise, was obtained a month later.

The programme was unfortunately cut short in February 1996 when a gyro failed on IUE, limiting observations to objects for which a bright (V<8) guide star was available. This was not the case for any of our remaining targets.

Two spectra were affected by the so-called '159DN anomaly' (see Table 2). A number of pixels were assigned the flux value 159DN when they should in fact have had a higher value. However, on close inspection it was found that only a small fraction of each of these two spectra was contaminated, and their scientific usefulness was not compromised.

3 IUE DATA REDUCTION

All of the spectra have been processed with NEWSIPS (New Spectral Image Processing System). NEWSIPS spectra contain a number of significant geometrical and photometric corrections which enhance spectral signal-to-noise and improve the photometric reliability of the data (e.g. a correction for the degradation of the detector with time, Bohlin and Grillmair 1988). Recent analysis by Garhart (1997) shows that, since 1993, the SWP camera sensitivity has in fact degraded at a rate greater than predicted, so that the current NEWSIPS calibration underestimates the SWP fluxes by up to 5%. Archival IUE data from 1993-96 are now being reprocessed to include a new degradation correction. However, this data was not available to us when we were preparing this paper, although we would expect the effect of the new calibration to be relatively minimal on the determination of any white dwarf parameters (for example, the errors on the flux values for the RE J0500−364 IUE SWP data are typically of order ∼10% anyway).

4 ANALYSIS

The method used to analyse the far-UV and EUV data for the hidden white dwarfs and the active stars detected and observed during this search has been discussed in detail in Paper I (Burleigh, Barstow and Fleming 1997). A summary is given here.

4.1 Hidden white dwarfs - far-UV data

In binary systems like these, it is not possible to use the H Balmer line profiles to measure temperature and gravity. However, the IUE SWP spectra can be used to estimate these parameters by matching the observed Lyman α profile and the UV continuum (the region uncontaminated by the companion) with synthetic spectra. Unfortunately, it is not possible to get an unambiguous determination of T and log g from a single spectral line. Instead, a range of possible models is determined by stepping through values of the surface gravity, from log g=7.0 to 9.0, and finding the best fit temperature and normalisation at each point.

We compare the observed far-UV data with fully line blanketed, homogeneously mixed H+He, LTE model atmospheres, spanning a temperature range from 20,000K to 100,000K, and kindly supplied by Detlev Koester (e.g. Koester 1991). In this analysis, we assume the white dwarfs have pure hydrogen envelopes. The spectral fitting is conducted with the XSPEC programme (Schafer et al. 1991), which calculates a chi-squared statistic for the fit between the data and the model, and which is then minimised by incremental steps in the free parameters. There is no need to take into account any interstellar component in the analysis of the Lyman α profile, because for columns greater than a few $\times 10^{19}$ the white dwarf is unlikely to be detected in EUV surveys.

The white dwarf radius and mass are calculated using the temperature-dependent evolutionary models of Wood (1995), which assume thick ($10^{-4} M_{\odot}$) H layers, and the radii are then used to estimate the distance from the model normalisation parameter (which is actually the solid angle of the star, equivalent to [radius/distance]^2). The distances to the primaries in each case can be calculated from the spectral type and V magnitude, and are given in Table 3. The range of white dwarf temperatures and gravities that give the best match to the distance of the primary can then be estimated. The V magnitude of each white dwarf is estimated from the model flux at 5500Å, and given in Table 5.

4.2 Hidden white dwarfs - ROSAT data

Once the temperature and gravity of each white dwarf has been estimated, the ROSAT EUV and soft X-ray fluxes can give an indication of the level of photospheric opacity in the stellar atmosphere, by comparing them with predicted values for a pure H model. The ROSAT data is fitted independently from the IUE data since contamination from elements heavier than H and He only has an effect at EUV and soft X-ray wavelengths. We fit the data from the two WFC filters, and the integrated count rate in the 0.1−0.28 keV PSPC band, within which all the white dwarf soft X-ray flux is expected to lie. It is possible that some EUV and X-ray emission might also originate from the normal stars in each system. Any detected PSPC flux at energies above 0.4 keV is an indication of the presence of an active companion (Table 6).

Once again we utilise Detlev Koester's fully line blanketed H+He models. These assume a homogenous distribution of hydrogen and helium, under LTE conditions, in the range $-8<$logHe/H<-3. The temperature, gravity and normalisation, estimated from the fit to the IUE data, are frozen during the modelling, but the He/H ratio is allowed to vary. The interstellar HI column density is also estimated by assuming that the local ISM is not highly ionised (i.e. there is minimal HeII absorption) and that the HeI/H ratio is cosmic (0.1).

The fitting is again conducted using the XSPEC programme. We consider a good fit to the data to correspond to the probability that a particular value of the reduced χ^2 (${\chi_r}^2$) can occur by chance to be 0.1 or greater (i.e. 90% confidence), and a bad fit 0.01 or less (99% confidence). The fits in between might not be very good, but cannot be ruled out with high confidence. In this analysis a good fit requires ${\chi_r}^2<2.71$, but until it exceeds 6.63 a model cannot be excluded with any certainty. Consequently, we list all model fits to the data for which ${\chi_r}^2<6.63$ (Table 6).

4.3 Non-detections and active stars

A number of the stars observed with IUE where no white dwarf was detected are probably coronally and chromospherically active. Some of these stars are also comparatively hard X-ray sources (i.e. they are detected in the 0.4−2.4 keV band of the ROSAT PSPC), and in some of the IUE LWP spectra chromospheric MgII emission was seen at 2798Å.

In these cases, estimates of the L_{EUV}/L_{bol} and L_x/L_{bol} ratios have been made as an indicator of the level of activity (Table 7). We adopt the methods outlined by Jeffries (1995) and Fleming et al. (1995) to estimate these parameters.

Where chromospheric MgII emission was seen the line fluxes above the continuum level were measured using a simple Gaussian profile, fitted to each line, after the continuum had first been subtracted (the continuum flux was represented by a low degree polynomial). Note that in each case the MgII emission actually fills-in an underlying absorption dip. However, it is impossible to estimate the depth of this absorption line, and thus the measurements presented here are only lower limits. The measured MgII fluxes are listed in Table 7, and have been used to estimate L_{MgII}/L_{bol}.

5 DISCUSSION

5.1 Hidden white dwarf binaries

5.1.1 RE J0500−364

The field of this EUV source (see Figure 1) was surveyed by Mason et al. (1995) during the WFC optical identification programme. No evidence of activity was found in the cores of Ca II H & K in the spectrum of a ∼13th magnitude star located at the centre of the source error box. Various stars were also examined outside the error box, but none could plausibly account for the EUV emission. The field was also examined on 1995 September 29/30 with the 2.3m Steward Observatory telescope on Kitt Peak, as part of a programme to search for the optical counterparts to unidentified sources in the ROSAT WFC 2RE catalogue. A spectrum (Figure 2) of the central star in the source error box was obtained with the Boller and Chivens Spectrometer and 800×1200 blue sensitive CCD. A 2.5" slit and 600 lines/mm grating blazed at 3658Å were used, and the data were reduced with standard IRAF routines. Again, there was no evidence for activity. One untested proposition was that this central object could be hiding a hot white dwarf companion. Therefore, the star was added to our IUE target list for observations during 1995/96, and a faint, ≈18th magnitude hot white dwarf companion was discovered (Figure 3).

By comparing the relative line strengths and widths of the primary's optical spectrum with spectra in the atlas of Jacoby, Hunter and Christian (1984), we conclude that it most closely resembles an F6/7V. It should be noted that the spectrum appears to be deficient in flux at the blue end, below ∼4500Å. As the star was observed at a relatively high air mass (sec Z=2.94), this deficiency in counts was probably caused by differential atmospheric dispersion. The spectral identification is strengthened when the IUE LWP spectrum (LWP31729, Figure 4) is compared to spectra in the IUE Spectral Atlas (Wu et al. 1991). The data are very noisy, and have been binned up as a consequence, but most closely match stars in the range F5V−G0V. There also appears to be a slight excess of flux in the IUE SWP spectrum, at wavelengths >1850Å, above the level expected from the white dwarf (Figure 3). If the excess is real, then it must attributable to the primary. As ∼13th magnitude mid-late G and K stars are not bright enough to be detected by IUE in this region of the spectrum, this also indicates that the companion is probably a late F. Taking the Guide Star Catalogue magnitude of V=13.29, the system lies between 755 (F7V) and 870 (F6V) parsecs away, although if we consider possible errors on the GSC magnitude (±0.3 mags), and that the absolute magnitudes may be in error by up to ±0.5 magnitudes, the system could be as close as 520 parsecs or as distant as 1250 parsecs.

Is this a true binary or a chance alignment? Given that the source of the EUV radiation is almost certainly the hot white dwarf, we can calculate the probability of a random 13th magnitude star also falling within the IUE aperture. According to Allen (1973), the number of stars per square degree at the Galactic latitude of RE J0500−364, brighter than V=13, is 87.1. The IUE large aperture is a 10"×20" oval, hence we calculate a probability of ≈1/250 of a chance alignment. (Note that the point spread function of the stellar image of the 13th magnitude star on the Digitised Sky Survey plate is ∼15" in radius, see Figure 1).

Assuming this is indeed a true binary, then we believe RE J0500−364 to be one of the most distant white dwarfs, if not the most distant, to be identified in the EUV surveys (for a comparison, see the distance estimates for the white dwarfs detected by the ROSAT PSPC by Fleming et al. 1996, and those detected by EUVE by Vennes et al. 1997b).

A model fit to the IUE spectrum at log g=7.25 gives T=38,260K and M=0.40M$_\odot$, corresponding to a distance of 830 parsecs. A fit at log g=8.0 corresponds to the minimum distance estimate to the system, but gives a higher mass, M=0.68M$_\odot$ and higher temperature, T=45,000K (and brings the star into the regime where its atmosphere may be contaminated by elements heavier then He). The inferred V magnitude from these models is 17.9, making this one of the faintest white dwarfs to be detected by ROSAT. The faintest, RE J0616−649 (V=18.4), is a rare magnetic DA

(Jordan 1997), but there are few other hot white dwarfs detected fainter than 17th magnitude.

This source is not included in the ROSAT PSPC All-Sky Survey Bright Source Catalogue (Voges et al. 1996), but it has been observed and detected in X-rays during a pointed observation by the ROSAT High Resolution Imager (HRI). The target was observed as part of programme to identify possible isolated neutron star candidates in the ROSAT surveys (PI Wang). Using the Point Source Search programme (PSS) within the STARLINK Asterix X-ray analysis package (see Pye et al. 1995) to analyse the HRI image, the position of the X-ray source was found to be coincident with the WFC and EUVE detections (Figure 1), and has a flux of 27.4±3.9 counts per 1000 sec^{-1}. The source shows no evidence for time variability.

Although the HRI has very limited spectral response (the spectral properties of the HRI are known to vary with detector position and time in an ill-defined manner), it is possible to obtain a crude hardness ratio. In this case, the HRI data can then be used to test whether there is any hard X-ray emission from the F6/7V companion star, since no emission is expected from the white dwarf photosphere above 0.4 keV. Figure 5 shows the HRI data plotted as a function of pulse height distribution. The exact energy of each channel varies temporarily and spatially, but channels 1 to 5 are roughly equivalent to the soft (0.1−0.4 keV) PSPC band, and channels 6−16 are equivalent to the hard (0.4−2.4 keV) band. As with the PSPC, a hardness ratio can be defined by (Hard−Soft)/(Hard+Soft). In this case, the hardness ratio =−1.0 confirming, as can be readily seen in Figure 5, that this is a very soft source. We conclude that all of the EUV and soft X-ray emission originates from the hot white dwarf.

Unfortunately, there is no reliable detector matrix for the HRI, and it did not prove possible to use the X-ray count rate in the subsequent analysis. Therefore, since this left only the two ROSAT WFC data points to try to constrain the interstellar hydrogen column density and white dwarf atmospheric parameters, we assumed that the white dwarf photosphere was essentially pure hydrogen (a reasonable assumption for T<40,000K, and for many hot DAs T<50,000K), and allowed only the neutral hydrogen column density to vary in the subsequent fitting of the EUV data. We found that the WFC S2 photometric data point is well matched by a model fit at log g=7.25, although the S1 flux was predicted to be slightly lower than observed. The hydrogen column density given by this model is $N_H=7.5\times10^{18}$ atoms cm^{-2}. At 830 parsecs distance, this translates into a neutral hydrogen line-of-sight volume density of only 0.0029 atoms cm^{-3}, well below the average local volume density within ∼80pc of the Sun of 0.05 atoms cm^{-3} (Warwick et al. 1993). If the system is closer (530 parsecs) and the log g=8.0 model is applied, then the H column density is higher ($N_H=2.4\times10^{19}$ atoms cm^{-2}) and the line-of-sight volume density is also higher at 0.0146 atoms cm^{-3}. Again, though, this is well below the average local volume density.

Notably, this system (galactic co-ordinates l=239.6°, b=−37.2°) lies in a similar direction to the known exceptionally low column densities towards the B1 giant β CMa (l=226°, b=−14°, Welsh 1991), and in particular to two other ROSAT-discovered hot white dwarfs, RE J0457−281 and RE J0503−289 (l=229.3°, b=−36.2°, Barstow et al. 1993).

At ≈200pc distance, β CMa is known to exist in a rareified "interstellar tunnel" of very low neutral gas density, which is itself an extension of the region surrounding the Sun called the Local Bubble (Welsh 1991). The features of the Bubble were first mapped out by Frisch and York (1983), and Welsh (1991) speculates that the β CMa tunnel may extend for *at least* 300pc in that direction away from the Sun. Welsh (1991) also estimates the tunnel to be about 50pc in diameter; the white dwarfs RE J0457−281 and RE J0503−289 (which are much closer at ≈90pc) may then possibly exist in a southward extension of this tunnel, or more likely lie in the foreground, within the Local Bubble itself.

Table 8 details the known column densities and volume densities to these three stars, and also to ϵ CMa (B2 II, l=239.8°, b=−11.3°), the brightest EUV source in the sky (Cassinelli et al. 1995), which lies in a similar direction. The line-of-sight neutral hydrogen volume density we measure for RE0500−364 compares favourably with the average volume density to these four stars (0.0030 atoms cm^{-3}). This suggets that RE J0500−364 might also lie within the β CMa extension of the Local Bubble.

If RE J0500−364 really does lie as far as ∼500 or more parsecs away, then it presents a possible lower limit to the size of any neutral gas-free corridor stretching away from the Local Bubble in that direction. The region is bounded on three sides by several OB associations: the Orion nebula (450pc away), the CMa OB1 association (800pc distant), and the Gum Nebula (290pc away). Welsh (1991) hypothesises that this tunnel may have been evacuated by a number of supernova explosions in the last few $\times10^5$ years. The injection of driven, heated, rarefied gas into an older (∼10^7 years old) low density cavity in the local interstellar medium would produce the large region of very low density neutral gas that we now see.

5.1.2 HD27483

The Hyades system HD27483 consists of two active F6V stars orbiting each other with a period of 3.05 days. Although an EUV source was detected originating from the direction of this system in the ROSAT WFC all sky survey in 1990, the hot white dwarf component was identified independently and serendipitously by Böhm-Vitense (1993) during an IUE SWP observation as part of a survey of Hyades F stars (Böhm-Vitense 1995). Böhm-Vitense (1993) derived atmospheric parameters for the white dwarf of 23000±1000K and $M=0.6M_\odot$. However, in the analysis of the white dwarf spectrum the author utilised the unblanketed models of Wesemael et al. (1980), assuming log g=8.0, to fit the far-UV spectrum at just two points. Since the white dwarf might be hot enough to be contributing to the observed EUV flux, it could be argued that the system should be included on the list of EUV-detected hidden white dwarfs, and thus we have decided to re-analyse the far-UV and ROSAT data here, in the same manner as the other recently discovered systems.

The ROSAT WFC source RE J0420+138, associated with HD27483, was listed in the original Bright Source Catalogue (Pounds et al. 1993), with a count rate of 15.0±4.0 counts ksec^{-1} (it was not detected in S2), but was not subsequently detected in the reprocessed 2RE survey (Pye et al. 1995). The significance of the S1 detection in the 2RE survey was 4.2; sources had to exceed a significance of 5.5 in a combination of both bands to be included in the catalogue. Even so, at T≈23,000K the white dwarf may be contributing to this small EUV flux, despite the fact that the two F star companions are known to be active themselves.

There is significant contamination in the IUE SWP spectrum (see Figure 6) at the long wavelength end from the two F6V star companions, but this falls to zero by 1600Å. Therefore, we were able to use the continuum flux up to this point. Böhm-Vitense estimated a distance of 47.6 parsecs to this system. We can further constrain this figure with the recently published *Hipparcos* parallaxes (ESA 1997), where the measured value for HD27483 is 21.8±0.85mas, corresponding to a distance of 45.9+1.80/−1.75 parsecs. The spectral model which best matches this distance has log g=8.5 and T=22,000, and the corresponding stellar mass is $M=0.94M_\odot$. The white dwarf age is then 1.4×10^8 years, in comparison with the age of the Hyades cluster, $\sim7\times10^8$ years (Böhm-Vitense 1993). Given that the white dwarf might have a higher mass than is the average for these stars ($\approx0.6M_\odot$, Marsh et al. 1997), we can estimate its progenitor mass and place a possible lower limit on the maximum mass for white dwarf progenitor stars in the Hyades cluster. From Wood (1992):

$$M_{WD}=\mathrm{A}\exp(\mathrm{B}\times M_{MS})$$

where $\mathrm{A}=0.49462M_\odot$ and $\mathrm{B}=0.09468{M_\odot}^{-1}$. We find, for $M_{WD}=0.94M_\odot$, $M_{MS}=6.7M_\odot$.

The main sequence lifetime of a $6.7M_\odot$ star is in fact significantly shorter than 560 million years (the difference between the Hyades age and the white dwarf cooling age, e.g. Schaller et al. 1992). This suggests that the white dwarf is, in reality, probably lower in mass than $0.94M_\odot$. However, in order to unambiguously and tightly constrain the fundamental parameters of this star, we will need to obtain a spectrum of the H Lyman series with an instrument such as the forthcoming *FUSE* mission (see also Section 6).

The WFC source is coincident with a ROSAT PSPC X-ray source, with a total count rate of 130.6±19.8 counts ksec^{-1}, including a detection in the upper band. This confirms that at least one of the two F6V companion stars is active, as the hard X-rays could not have originated from the white dwarf. The ROSAT data points cannot be matched with any of the white dwarf models (which assume a homogeneous atmospheric mixture of H and He). This implies that the active star(s) must be providing a significant fraction of the EUV flux, since little or no heavy element contamination is expected in the white dwarf photosphere in this cool temperature regime. It is even possible that there is no flux at all from the white dwarf at these wavelengths. The contribution of the white dwarf to the S1 count rate can, however, be estimated. Another hot WD+MS binary, V471 Tauri, is detected by ROSAT in the Hyades cluster (Barstow et al. 1992). After subtracting the contribution from the active K2V companion, Marsh et al. (1997) use the WFC count rates to estimate the H column density to this system (8.52×10^{18} atoms cm^{-2}). Adopting the same column density to HD27483, assuming a pure H atmosphere, and using the parameters derived from the log g=8.5 model, the white dwarf is predicted to contribute 5.4 counts ksec^{-1} to the S1 flux (i.e. ≈1/3 of the 15 counts ksec^{-1} detected). How is this count rate affected by uncertainties in the H column density? In fact, from EUVE spectra, Dupuis et al. (1997) derived a much lower H column density to V471 Tauri of 1.5×10^{18}. Using this value, in the log g=8.5 model, the white dwarf contributes 7.6 counts ksec^{-1} to the S1 flux (i.e. ≈1/2 of the observed flux). This hot degenerate companion to HD27483 could itself, then, be regarded as a real EUV source. At T≈22,000K, this would make it one of the coolest white dwarfs to be detected in the EUV surveys.

The combined X-ray luminosity of the two F6V stars in the HD27483 system can also be estimated, by subtracting the contribution of the white dwarf to the ROSAT PSPC lower band flux. The PSPC count rates are 98±14 counts ksec^{-1} in the softer 0.1−0.4keV band, and 33±9 counts ksec^{-1} in the harder 0.4−2.4keV band (Voges et al. 1996). In the log g=8.5 model, assuming a column density of 8.52×10^{18} atoms cm^{-2}, the white dwarf flux in the 0.1−0.4keV band is found to be 36.0 counts ksec^{-1}. Eliminating this from the total PSPC lower band rate and following the method detailed by Fleming et al. (1995), we find $L_x=1.7\times10^{29}$ ergs sec^{-1}, and $L_x/L_{bol}=7.8\times10^{-6}$.

5.2 Non-detections and active stars

5.2.1 *BD+49°646 (2RE J0222+50)*

This unclassified star was only observed by the SWP camera (SWP56333), and there was no flux visible above the background. If BD+49°646 is a G or K star, then we probably would not detect it in this waveband anyway. No emission features are visible in the UV spectrum, but the EUV source is coincident with a ROSAT PSPC hard X-ray source, and the possibility must remain that BD+49°646 is coronally active. Alternatively, the EUV/X-ray source might be another object in the field, or it is possible that the target was missed altogether in the IUE observation.

5.2.2 *2RE J0232−02*

As with the WD+MS binary RE J0500−364 (discussed above), the field of this WFC source was originally observed in 1995 with the 2.3m Steward Observatory telescope at Kitt Peak, as part of a programme to try to identify the remaining optical counterparts to unknown EUV sources in the ROSAT WFC catalogues. In the absence of any plausible EUV source, the 15th magnitude G-type central star in the error box may be hiding a hot white dwarf companion. The far-UV spectra obtained with IUE (SWP56272 and LWP31800) were very noisy and showed no evidence for a hot white dwarf. There was some flux above the background longwards of ∼2700Å in the LWP spectrum, which may have been due to a G star, but it is possible that the target was missed altogether, and this flux was due to scattered solar light which effects the LWP camera sporadically. At V=14.8 this star is unlikely to be the source of the EUV flux: a 15th magnitude main sequence mid-G star would require $L_{EUV}/L_{bol}\sim0.1$ to produce the count rate seen in the WFC S2 filter (45 counts ksec^{-1}), far in excess of the saturation level for coronal emission ($L_{EUV}/L_{bol}\sim10^{-3}$, Mathioudakis et al. 1995).

5.2.3 SAO150508 (2RE J0530−19)

Prior to the publication of the 2RE catalogue (Pye et al. 1995), the 9th magnitude F6V star SAO150508 was not thought to be active, although there are no published optical observations which might offer evidence one way or another. The IUE spectra (SWP 56195 and LWP31700, Figure 7) show no evidence for a hot white dwarf companion. SAO150508 is, however, coincident with a ROSAT PSPC X-ray source. Therefore, estimates of the X-ray and EUV luminosities, assuming SAO150508 is active and the true source of the EUV and X-ray flux, are presented in Table 7.

5.2.4 HD36869 (2RE J0534−15)

There is no evidence in the literature that the 8th magnitude G2V star HD36869 is active. The IUE spectra (SWP56169 and LWP 31701, Figure 8) also show no evidence for activity, although the star is coincident with a ROSAT PSPC source. Given that 8th magnitude stars are comparatively rare, it is still possible that HD36869 is coronally active, and thus we provide estimates of the X-ray and EUV luminosities in Table 7.

5.2.5 Gl216B (2RE J0544−22)

Gl216B (K2V) is part of a nearby (≈8 parsecs) triple system, and was chosen as a candidate white dwarf binary on the basis of the S2/S1 count rate ratio. The IUE spectra (SWP56194 & LWP31699, Figure 9) show no evidence for a hot white dwarf. However, Mg II 2798Å is visible in emission (with a line flux of $4.2\pm0.7\times10^{-12}$ ergs cm^{-2} s^{-1} above the continuum). The emission feature in the SWP spectrum at ∼1720Å is probably spurious, since it does not coincide with any commonly seen line. From observations made in the optical, de Strobel et al. (1989) concluded that this is a young, active star. If it is the only source of the EUV flux, then we determine $L_{EUV}/L_{bol}=2.78\times10^{-5}$.

Active stars have a characteristic EUV to Mg II flux ratio. For example, Jewell (1993) shows that the 0.05−0.2 keV EUV flux is 1−10 × the MgII flux. For Gl216B, though, the EUV to Mg II flux ratio is only ≈0.8.

Schmitt et al. (1990) observed the entire Gl216 system in an Einstein HRI pointing, and found that the nearby F7V star Gl216A was 8 times brighter in X-rays than Gl216B. Thus Hodgkin and Pye (1994) concluded that all of the EUV radiation in fact comes from Gl216A. However, we only targeted Gl216B with IUE since this is the object associated with the EUV source in the 2RE catalogue, and at the time of the observation we were unaware of Hodgkin and Pye's conclusion. The low EUV to Mg II flux ratio for Gl216B does, though, support these earlier conclusions that the major source of the EUV radiation is actually Gl216A.

Estimates of the X-ray and EUV luminosities are given in Table 7 assuming a) all the flux comes from Gl216A and b) all the flux comes from Gl216B.

5.2.6 HR2225 (HD43162, RE J0613−23)

This G5V star was not known to be active prior to the ROSAT survey, but subsequently it has been studied in detail by Jeffries and Jewell (1993) and is almost certainly the EUV source. It is also an X-ray source, and measurements of the X-ray and EUV luminosities are given in Table 7. No obvious emission features are visible in the IUE LWP and SWP spectra (Figure 10); the feature longwards of 1800Å in the SWP spectrum is probably spurious, as there is no commonly seen line at this wavelength.

5.2.7 HD295290 (2RE J0640−03)

There are no references in the literature to this being an active star. However, Mg II is clearly seen in emission at 2800Å in the IUE LWP spectrum (Figure 11), and there is a suggestion of CIV in emission at 1550Å in the short wavelength region. Measurements of the X-ray and EUV luminosities are given in Table 7 using the G0 classification given by SIMBAD, and assuming the star is on the main sequence. The EUV to Mg II flux ratio (≈8.0) strongly suggests that this star is active and the true source of the EUV radiation. Note that the ratios L_{EUV}/L_{bol} and L_x/L_{bol} are significantly larger than for any of the other stars in this sample, approaching the saturated level for coronal emission ($\sim10^{-3}$). This suggests that the star may be rapidly rotating.

5.2.8 HD54402, (2RE J0710+45)

No references are given in the literature to this being an active star. There is clearly no white dwarf visible in the IUE SWP spectrum (Figure 12), and the emission line at ∼1800Å is probably spurious, perhaps due to a cosmic ray hit. The EUV source is not coincident with an X-ray source. The star needs to be examined optically to search for any evidence of chromospheric activity.

5.2.9 SAO135659, (2RE J0813−07)

Again, this star was not known to be active prior to the ROSAT survey. The IUE LWP spectrum (Figure 13) reveals Mg II in emission at 2800Å. Measurements of the EUV and X-ray luminosities (this star is also a PSPC source) are given in Table 7, assuming the K0 spectral type given by SIMBAD, and that the star is on the main sequence. The EUV to Mg II flux ratio (≈8.25) strongly suggests that this star is active and the true source of the EUV radiation.

5.2.10 RE J0823−252/HD70907

With S1 and S2 count rates of 52±7 and 83±9 counts ksec^{-1}, this is a relatively bright EUV source in comparison with most of the targets in this paper. The soft X-ray and EUV photometric colours are also characteristic of a hot white dwarf, and it is not detected in the PSPC hard band. Therefore, it was selected as a potential hidden white dwarf binary.

The V=8.8 star in the centre of the field, HD70907 (F3IV/V), was observed in both the IUE SWP and LWP cameras (Figure 14). There is no evidence for a white dwarf companion or emission features indicative of an active star. A nearby V≈11 star was also observed and again there was no evidence for a white dwarf, although, in the absence of any flux in the LWP camera that could be attributed to a stellar source, it seems possible that the star was not in the

LWP slit. Mason et al. (1995) report that this fainter object is indeed active, although they give no indication of the size of any emission features seen in the optical. They also do not give a spectral type for this star, and thus we have not been able to determine the EUV and X-ray luminosities. Whether this star is active enough to be the true EUV source remains unclear, and the suspicion remains that there is indeed an unresolved hot white dwarf hiding in this field.

5.2.11 HR4646 (2RE J1212+77)

It is highly unusual to detect an A star in EUV or X-ray surveys (Fleming et al. 1991). Observations by the Einstein and EXOSAT observatories failed to find any convincing detections other than the nearby quadruple A star system Castor (Pallavicini et al. 1990). Therefore HR4646, an Am star coincident with ROSAT WFC 2RE and PSPC sources, was selected as a potential hidden white dwarf binary. It should be noted that Am stars do not possess significant magnetic fields and they are slow rotators, but they almost always appear to lie in close binary systems (Abt 1961), and indeed Margoni, Munari and Stagni (1992) found that HR4646 is a spectroscopic binary with a period of 1.27 days.

The IUE SWP spectrum (Figure 15) shows no evidence for a hot white dwarf companion. It is extremely likely, therefore, that HR4646 has a coronally active cooler companion (F5 or later).

6 SUMMARY AND CONCLUSIONS

A search for unresolved white dwarfs in binary systems with optically brighter normal stellar companions has been conducted with IUE during its final year of operation. Targets were chosen among the fainter and still un-identified EUV sources in the ROSAT 2RE catalogue (Pye et al. 1995). One new system was discovered (RE J0500−364, DA+F6/7V), which appears to lie in a direction of low interstellar neutral hydrogen volume density. If this star is really as distant as ∼500-1000pc, then it may represent a lower limit to the size of the β CMa tunnel of low density neutral gas stretching away from the Local Bubble in that direction.

Including the independently identified HD27483 (DA+F6V, Böhm-Vitense 1993), this new discovery brings the total number of such systems found in the ROSAT and EUVE surveys to nineteen. These two satellites have, therefore, been very successful in helping us to identify these kinds of binary systems, which have never been seen optically and could only have been identified through such satellite surveys. However, these stars still represent <20% of the hot white dwarfs identified in the EUV.

The demise of IUE, which suffered a gyro failure in February 1996, limiting it to observe only targets with bright guide stars (the mission was finally terminated in September 1996), effectively cut short our programme. The loss of IUE means that this particular method of searching for these important systems is no longer available. Although HST can observe the same wavelength region, it is of course much harder to obtain the time required for this kind of search. It is likely, therefore, that very few new examples of these systems will be discovered in the near future. The results presented in this paper seem to suggest that this search, using the EUV catalogues as a basis from which to identify potential systems, has been fairly exhaustive (we have identified only one new system from thirteen targets).

However, the identification by Vennes et al. (1997) of a hot white dwarf companion to a previously catalogued EUV-bright active star, RE J0702+129 (K0Ve), instead suggests that, in fact, some systems may have been completely overlooked. RE J0702+129 was classified as active by Mason et al. (1995) in their optical follow-up programme to identify the EUV sources found in the ROSAT WFC survey, and was not, therefore, included on any of our target lists for the IUE search. This raises the question of how many of the >200 'active' stars in the WFC and EUVE catalogues really are the source, or at least the only source, of the EUV radiation. Until each star has been observed and analysed in detail, the suspicion remains that there are more of these binary systems in the survey waiting to be identified.

For example, the ROSAT WFC catalogue includes ≈120 isolated white dwarfs, and ≈60 in some kind of binary, e.g. classic Sirius-type systems, CVs, non-interacting DA+dM systems, and visual binaries. Conservatively, then, we might assume that we have already identified the majority of the white dwarf binaries to be found in the survey. However, if as many as 80% of stars reside in binary or multiple systems, another 30 might be awaiting discovery. These could include double degenerate systems as well as further examples of Sirius-type systems (e.g. the apparently isolated DA RE J0512−007 has a mass, $M=0.38M_{\odot}$, too low for it to be the result of single star evolution, and may have a degenerate companion).

What is really needed to try to find more Sirius-type binaries is an all-sky UV survey. None has been undertaken since the TD-1 survey of 1972/73, which originally appeared to have only detected Sirius B among these systems. Subsequently, though, Landsman, Simon and Bergeron (1996) found white dwarf companions to 56 Persei and HR3643 as a result of the UV excess detected by TD-1. The recently approved *GALEX* mission (Bianchi 1998), which will survey the sky at UV wavelengths and follow-up some targets spectroscopically, may reveal many more of these binaries.

In the meantime, follow-up observations of these nineteen new EUV-bright systems are required. In particular, it is important to determine whether these systems are wide, or close enough that they must have undergone Common Envelope evolution. This information will help to place constraints on theoretical models of binary evolution (e.g. de Kool and Ritter 1993). Detailed studies of the normal stellar companions may also reveal evidence of past interaction (e.g. Jeffries and Stevens 1996), and stars with possible abundance anomalies that may be the progenitors of the Barium and Carbon giants (e.g. Jeffries and Smalley 1996).

In addition, the forthcoming *FUSE* mission (Far Ultraviolet Spectroscopic Explorer) will, for the first time, allow us to unambiguously determine the temperatures and surface gravities of the white dwarfs in these systems (and hence their masses and radii), through modelling of the H Lyman absorption series down to 912Å.

ACKNOWLEDGEMENTS

MRB and MAB acknowledge the support of PPARC, UK. We wish to thank Detlev Koester (Kiel) for the use of his white dwarf model atmosphere grids, and Jim Collins (Arizona) and Nigel Bannister (Leicester) for their help in obtaining and reducing the optical spectrum of RE J0500−364. MRB wishes to thank the staff at IUE Vilspa for their help and co-operation in carrying out this programme. We also thank the referee, Rob Jeffries, for useful suggestions to improve this paper. This research has made use of the SIMBAD database operated at CDS, Strasbourg, France, and data obtained from the Leicester Database and Archive Service (LEDAS) at the Department of Physics and Astronomy, Leicester University, UK.

REFERENCES

Abt H.A., 1961, ApJS, 6, 37
Allen C., 1973, *Astrophysical Quantities*, Athlone Press, London
Barstow M.A., Schmitt J.H.M.M., Clemens J.C., Pye J.P., Denby M., Harris A.W., Pankiewicz G.S., 1992, MNRAS, 255, 369
Barstow M.A. et al., 1993, AdSpR, 131, 281
Barstow M.A. et al., 1994, MNRAS, 270, 499
Bianchi L., 1998, in: Ultraviolet astrophysics − Beyond the IUE final archive, ESA publication SP−413, 797
Böhm-Vitense E., 1980, ApJ, 239, L79
Böhm-Vitense E., 1993, Astron J., 106, 1113
Böhm-Vitense E., 1995, AJ, 110, 228
Bohlin R.C., Grillmair C.J., 1988, ApJS, 66, 209
Bowyer S. et al., 1994, ApJS 93, 569
Bowyer S. et al., 1996, ApJS, 102, 129
Burleigh M.R., Barstow M.A., 1997, in: White Dwarfs, eds. J. Isern, M. Hernanz and E. Garcia-Berro, Kluwer, 329
Burleigh M.R., Barstow M.A., 1998, MNRAS, 295, L15
Burleigh M.R., Barstow M.A., Fleming T.A., 1997, MNRAS, 287, 381 (Paper I)
Cassinelli J.P. et al., 1995, ApJ, 438, 932
Cassinelli J.P. et al., 1996, ApJ, 460, 949
Dupuis J., Vennes S., Chayer P., Cully S., Rodriguez-Bell T., 1997, in: White Dwarfs, eds. J. Isern, M. Hernanz and E. Garcia-Berro, Kluwer, 277
ESA, 1997, *The Hipparcos Catalogue*, ESA SP−1200
Fleming T.A., Liebert J., Green R.G., 1986, ApJ, 308, 176
Fleming T.A., Schmitt J.H.M.M., Barstow M.A., Mittaz J.P.D., 1991, A&A, 246, L47
Fleming T.A. et al., 1995, ApJS, 99, 701
Fleming T.A., Snowden S.L., Pfefferman E., Briel U., Greiner J., 1996, A&A, 316, 147
Frisch P.C., York D.G., 1983, ApJ, 271, L59
Garhart M., 1997, IUE Newsletter (GSFC) Vol. 5, No. 5
Hodgkin S.T., Barstow M.A., Fleming T.A., Monier R., Pye J.P., 1993, MNRAS, 263, 229
Hodgkin S.T., Pye J.P., 1994, MNRAS, 267, 840
Koester D., 1991, IAU Symposium 145, Evolution of Stars: The Photospheric Abundance Connection, eds. G. Michaud and A. Tutukov, Kluwer Dordrecht, 435
de Kool M., Ritter H., 1993, A&A, 267, 397
Jacoby J.H., Hunter D.A., Christian C.A., 1984, ApJS, 56, 257
Jeffries R.D., Jewell S.J., 1993, MNRAS, 264, 106
Jeffries R.D., Burleigh M.R., Robb R.M., 1996, A&A, 305, L45
Jeffries R.D., Stevens I.R., 1996, MNRAS, 279, 180
Jeffries R.D., Smalley B., 1996, A&A, 315, L19
Jewell S.J., 1993, PhD Thesis, University of Birmingham
Johnson H.R., Ake T.B., 1986, ESA SP-263, 395
Jordan, S., 1997, in: White Dwarfs, eds. J. Isern, M. Hernanz and E. Garcia-Berro, Kluwer, 397
Landsman W., Simon T., Bergeron P., 1996, PASP, 108, 250
Margoni R., Munari U., Stagni R., 1992, A&AS, 93, 545
Marsh M.C. et al., 1997, MNRAS, 286, 369
Mason K.O. et al., 1995, MNRAS, 274, 1194
Mathioudakis M., Fruscione A., Drake J.J., McDonald K., Bowyer S., Malina R.F., A&A, 300, 775
McCook G.P. and Sion E.M., 1998, ApJS, in preparation
Pallavicini R., Tagliaferri G., Pollock A.M.T., Schmitt J.H.M.M., Rosso C., 1990, A&A, 227, 483
Pounds K.A. et al., 1993, MNRAS, 260, 77
Pye J.P. et al., 1995, MNRAS, 274, 1165
Schindler M., Stencel R.E., Linsky J.L., Basri G.S., Helfand D.J., 1982, ApJ, 263, 269
Schafer R.A. et al., 1991, ESA TM-09
Schaller G., Schaerer D., Meynet G., Maeder A., 1992, A&AS, 96, 269
Schmitt J.H.M.M., Collura A., Sciortino S., Vaiana G.S., Harnden F.R., Rosner R., 1990, ApJ, 365, 704
Shipman H.L., Geczi J., in 'White Dwarfs', ed. G. Wegner, Springer-Verlag, 134
Vennes S., Mathioudakis M., Doyle J.G., Thorstensen J.R., Byrne P.B., 1995, A&A, 299, L29
Vennes S., Berghoefer T., Christian D.J., 1997, ApJ, 491, L85
Vennes S., Christian D.J., Mathioudakis M., Doyle J.G., 1997, A&A, 318, L9
Vennes S., Thejll P.A., Genova Galvan R., Dupuis J., 1997b, ApJ, 480, 714
Voges W., et al., 1996, IAU Circ. 6420
Warwick R.S., Barber C.R., Hodgkin S.T., Pye J.P., 1993, MNRAS, 262, 289
Welsh, B.Y., 1991, ApJ, 373, 556
Wesemael F., Auer L.H., van Horn H.M., Savedoff M.P., 1980, ApJS, 43, 159
Wood M.A., 1992, ApJ, 386, 539
Wood M.A., 1995, in Proc. of the 9th European Workshop on White Dwarfs, eds. D. Koester and K. Werner, Springer, 41
Wu C.-C. et al., 1992, *IUE* Ultraviolet Spectral Atlas of Selected Astronomical Objects, NASA Reference Publication 1285

FIGURE CAPTIONS

Figure 1: Field of the ROSAT WFC EUV source RE J0500−364 (6×6 arcmins). The circles are the 90% error boxes, centred on the source co-ordinates, of (in order of decreasing size) EUVE, the WFC, and the ROSAT HRI. The WFC error box is centred on co-ordinates (J2000) 05 00 03.9 −36 24 02. The DA+F6/7V binary lies near the centre of each error box. The arrows indicate other stars examined by Mason et al. (1995) and ourselves during optical searches for the EUV and X-ray counterpart. None of these objects was particularly remarkable.

Figure 2: Optical spectrum of RE J0500−364 obtained with the Steward Observatory 2.3m telescope on Kitt Peak. Using this spectrum, we classify the star as F6/7V.

Figure 3: Far-ultraviolet IUE SWP spectrum of RE J0500−364 (SWP56217), obtained in December 1995 (8 hour exposure), clearly showing the white dwarf companion. Also shown is a pure H model atmosphere fit for log g=7.25, T=38,260K and M=0.40$M_\odot$.

Figure 4: Far-ultraviolet IUE LWP spectrum of RE J0500−364 (LWP31729). The data are very noisy and have been binned up, but the spectral shape most closely matches stars in the range F5V−G0V, consistent with the optical data.

Figure 5: Pulse height distribution of the X-rays from RE J0500−364 detected by the ROSAT HRI. Although the exact energies of each channel are known to vary spatially and temporally, it can be seen that this is a soft source, and there are no hard counts.

Figure 6: Far-ultraviolet IUE SWP spectrum of HD27483 (SWP45940). The hot white dwarf can clearly be seen emerging from the glare of the two F6V companions shortwards of ∼1700Å. Also shown is a pure H model atmosphere fit for log g=8.5, T=22,000K and M=0.94$M_\odot$.

Figure 7: Far-ultraviolet IUE spectrum of SAO150508 (G5V, SWP56195+LWP31700). Clearly, there is no white dwarf companion to this star.

Figure 8: Far-ultraviolet IUE spectrum of HD36869 (G2V, SWP56169+LWP31701). No white dwarf companion is visible in the short wavelength spectrum.

Figure 9: Far-ultraviolet IUE spectrum of Gl216B (K2V, SWP56194+LWP31699). Mg II 2798Å is visible in emission. The feature at ∼1720Å (inset) is probably due to a cosmic ray hit.

Figure 10: Far-ultraviolet IUE spectrum of HR2225 (G5V, SWP56206+LWP31715). The emission feature at ∼1800Å (inset) is probably spurious.

Figure 11: Far-ultraviolet IUE spectrum of HD295290 (G0V, SWP56211+LWP31726). MgII is clearly seen in emission at 2798Å. CIV 1549Å emission is also suggested in the SWP spectrum (inset).

Figure 12: Far-ultraviolet IUE spectrum of HD54402 (K0, SWP56193+LWP31698). The feature at ∼1800Å is probably due to a cosmic ray hit.

Figure 13: Far-ultraviolet IUE spectrum of SAO135659 (K0, SWP56273+LWP31801). MgII is visible in emission at 2798Å.

Figure 14: Far-ultraviolet IUE spectrum of HD70907 (F3IV/V, SWP56344+LWP31836). There is no evidence for activity.

Figure 15: Far-ultraviolet IUE SWP spectrum of HR4646 (A5m, SWP55658). Clearly, there is no white dwarf companion to this star.

Table 1. ROSAT WFC/PSPC and EUVE count rates ($1000s^{-1}$)

ROSAT No.	Name‡	WFC S1	WFC S2	PSPC (0.1−0.4keV)	PSPC (0.4−2.4keV)	EUVE 100Å	EUVE 200Å
WD Binaries							
RE J0500−36[a]		20±5	47±8	no det.	no det.	21±6	no det.
RE J0420+13[b]	HD27483	15±4	27†	98±14	33±9	no det.	no det.
Non-WD Systems							
2RE J0222+50	BD+49°646	14±3	17±5	258±20	195±18	no det.	no det.
2RE J0232−02		15†	45±11	no det.	no det.	no det.	no det.
2RE J0530−19	SAO150508	8±3	16±5	159±18	195±20	no det.	no det.
2RE J0534−15	HD36869	8±3	19±5	221±22	217±22	no det.	no det.
2RE J0544−22	Gl 216B	7±3	22±5	261±23	82±13	no det.	no det.
RE J0613−23	HR2225	18±3	35±9	517±30	256±21	no det.	no det.
2RE J0640−03	HD295290	9±3	32±8	304±28	281±27	no det.	no det.
2RE J0710+45	HD54402	8±3	26±7	no det.	no det.	no det.	no det.
2RE J0813−07	SAO135659	14±6	55±16	207±35	195±34	no det.	no det.
RE J0823−25[c]		52±7	83±9	175±24	no det.	28±11	no det.
2RE J1212+77	HR4646	13†	18±5	157±42	114±36	no det.	no det.

† upper limit
a] Detected in the First EUVE Source Catalog only (Bowyer et al., 1994)
b] ROSAT WFC Bright Source Catalogue detection only (Pounds et al., 1993)
c] HD70907 and a V≈11 companion were both observed as possible counterparts to this source

Table 2. Log of IUE observations

Name	SWP No.	LWP No.	Date	Exp. (s)	Observer	notes
WD Binaries						
RE J0500−364	56217		1995/323	1800	SO	
	56338		1995/358	29400	SO	159DN problem
		31729	1995/323	1800	SO	
HD27483	45940		1992/273	2100	Böhm-Vitense	
Non-WD systems						
2RE J0222+50	56333		1995/358	1800	SO	
2RE J0232−02	56272		1995/340	1800	SO	
		31800	1995/340	1800	SO	
SAO150508	56195		1995/317	1800	SO	
		31700	1995/317	1200	SO	
HD36869	56196		1995/317	1800	SO	
		31701	1995/317	360	SO	
Gl216B	56194		1995/317	1800	SO	
		31699	1995/317	120	SO	
HR2225	56206		1995/319	1800	SO	
		31715	1995/319	60	SO	
HD295290	56211		1995/322	1800	SO	
		31726	1995/322	1200	SO	159DN problem
HD54402	56193		1995/317	1800	SO	
		31698	1995/317	300	SO	
SAO135659	56273		1995/340	1800	SO	
		31801	1995/340	1200	SO	
HD70907	56344		1995/359	1800	SO	
		31836	1995/359	300	SO	
RE J0823−25†	56266		1995/338	1800	SO	
		31796	1995/338	300	SO	
HR4646	56393		1996/009	100	SO	

SO= Service Observation
† V≈11 companion to HD70907

Table 3. Physical parameters of the companion stars in the WD binaries

RE No.	Cat. Name	SpT	V	d est. (pc)	references
RE J0500−36		F6/7V	13.7	520−1250	
RE J0420+13	HD27483	F6V	6.17	47.6	Böhm-Vitense (1993)

Table 4. Physical parameters of the stars observed where no white dwarf was detected

RE No.	Cat. Name	Spectral type	V magnitude	references
2RE J0222+50	BD+49°646	?	10.1	SIMBAD
2RE J0232−02		K	14.8	SIMBAD
2RE J0530−19	SAO150508	G5V	9.0	SIMBAD
2RE J0534−15	HD36869	G2V	8.0	SIMBAD
2RE J0544−22	Gl216B	K2V	6.15	SIMBAD
RE J0613−23	HR2225	G5V	6.39	SIMBAD
2RE J0640−03	HD295290	G0	9.1	SIMBAD
2RE J0710+45	HD54402	K0	7.7	SIMBAD
2RE J0813−07	SAO135659	K0	8.8	SIMBAD
RE J0823−25	HD70907	F3IV/V	8.8	SIMBAD
		late	11	Mason et al. (1995)
2RE J1212+77	HR4646	A5m	5.14	SIMBAD

Table 5. Temperatures and gravities for the white dwarfs from homogeneous model fits

Binary	log g	Temp K	90% error K	Mass $M_\odot$	Radius $R_\odot$	d_{wd} (pc)	Estimated V
RE J0500−36	7.0	36,800	33,900-41,000	0.38	0.032	1050	17.8
	7.25	38,260	35,350-42,900	0.40	0.025	830	17.9
	7.5	42,000	36,400-45,700	0.47	0.020	740	17.9
	8.0	45,000	40,500-50,500	0.68	0.014	520	17.9
	8.5	50,500	45,400-57,700	0.97	0.009	390	18.0
	9.0	60,500	51,900-67,500	1.21	0.006	270	18.1
HD27483	7.0	20,000	upper limit	0.37	0.032	103	13.9
	7.5	20,000	upper limit	0.40	0.019	61	13.9
	8.0	21,410	21,215-21,630	0.63	0.013	50	14.2
	8.5	22,000	21,910-22,780	0.94	0.009	44	14.5
	9.0	24,800	24,570-25,060	1.20	0.006	30	14.6

Table 6. Column densities from homogeneous models for RE J0500−362 (assuming pure H composition)

Name	log g	T	HI column	90% error	Comment
RE J0500−364	7.0	36,800	3.7×10^{18}	$1.7-7.0\times10^{18}$	
	7.25	38,260	7.5×10^{18}	$5.0\times10^{18}-1.1\times10^{19}$	
	7.5	42,000	1.7×10^{19}	$1.4-2.1\times10^{19}$	
	8.0	45,000	2.4×10^{19}	$2.1-2.9\times10^{19}$	
	8.5	50,500	-	-	No fit
	9.0	60,500	-	-	No fit

No fit could be obtained to the ROSAT data for HD27483

Table 7. EUV and X-ray luminosities for the probable and confirmed active stars

Name	d(pc)	L_{EUV} $\times10^{29}$ ergs	L_{EUV}/L_{bol} $\times10^{-4}$	L_x $\times10^{29}$ ergs	L_x/L_{bol} $\times10^{-4}$	f_{MgII} $\times10^{-12}$	L_{MgII}/L_{bol} $\times10^{-4}$
SAO150508	59	10.0	3.6	1.3	4.7	-	-
HD36869	48	7.9	1.7	10.0	2.2	-	-
Gl216A	8	0.3	0.04	0.2	0.02	-	-
Gl216B	8	0.3	0.3	0.2	0.2	4.2	0.5
HR2225	18	2.0	0.7	2.0	0.7	-	-
HD295290	95	51.8	8.2	51.5	8.2	0.6	1.0
SAO135659	34	11.4	0.7	4.5	0.4	1.0	1.1

Table 8. Neutral hydrogen column and volume densities in the local interstellar medium

Name	l	b	d(pc)	N_H (cm^{-2})	nH (cm^{-3})	Ref.
β CMa	226.1	−14.3	206	$2.2\times10^{18\dagger}$	0.0035	Cassinelli et al. 1995
ϵCMa	239.8	−11.3	188	$1.2\times10^{18\dagger}$	0.0021	Cassinelli et al. 1996
RE J0457−281	229.3	−36.2	90	9.6×10^{17}	0.0035	Barstow 1997 *private com.*
RE J0503−289	230.7	−34.9	90	8.2×10^{17}	0.0030	Barstow 1997 *private com.*
RE J0500−364	239.6	−36.2	830	7.5×10^{18}	0.0029	this paper

† Upper limit

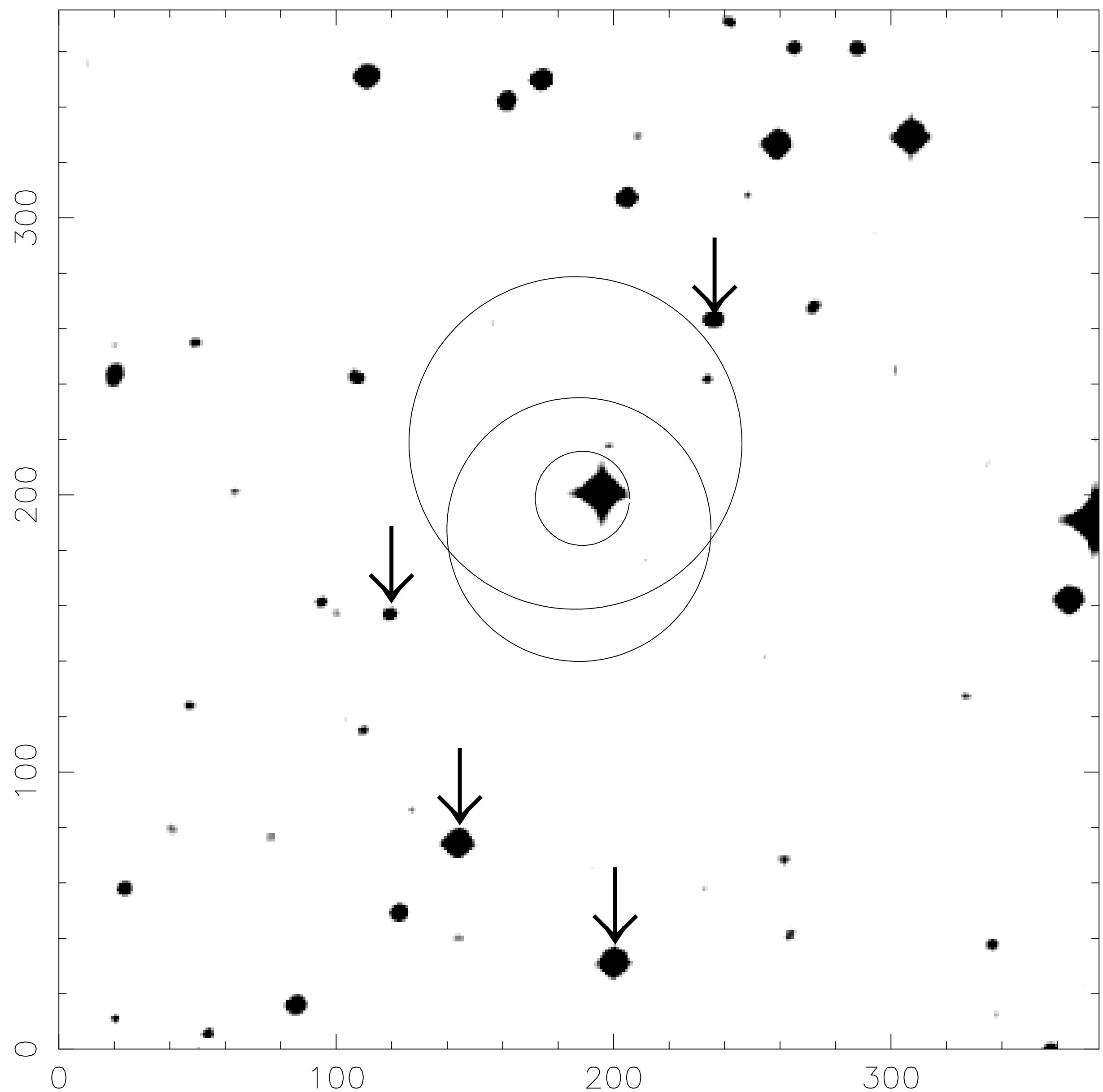

0
100
200
300

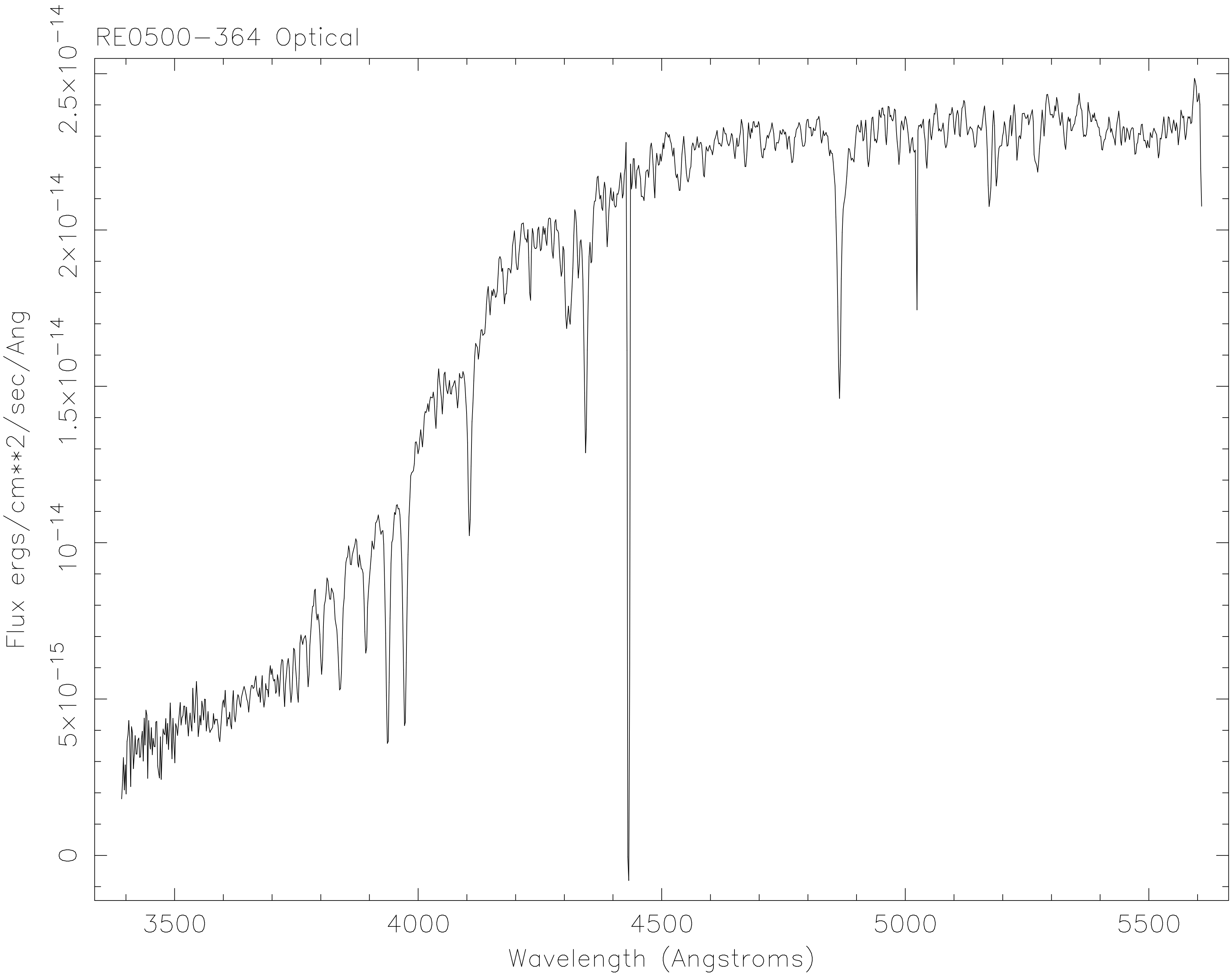
RE0500-364 Optical
Flux ergs/cm**2/sec/Ang
2.5×10⁻¹⁴
2×10⁻¹⁴
1.5×10⁻¹⁴
10⁻¹⁴
5×10⁻¹⁵
0
3500
4000
4500
5000
5500
Wavelength (Angstroms)

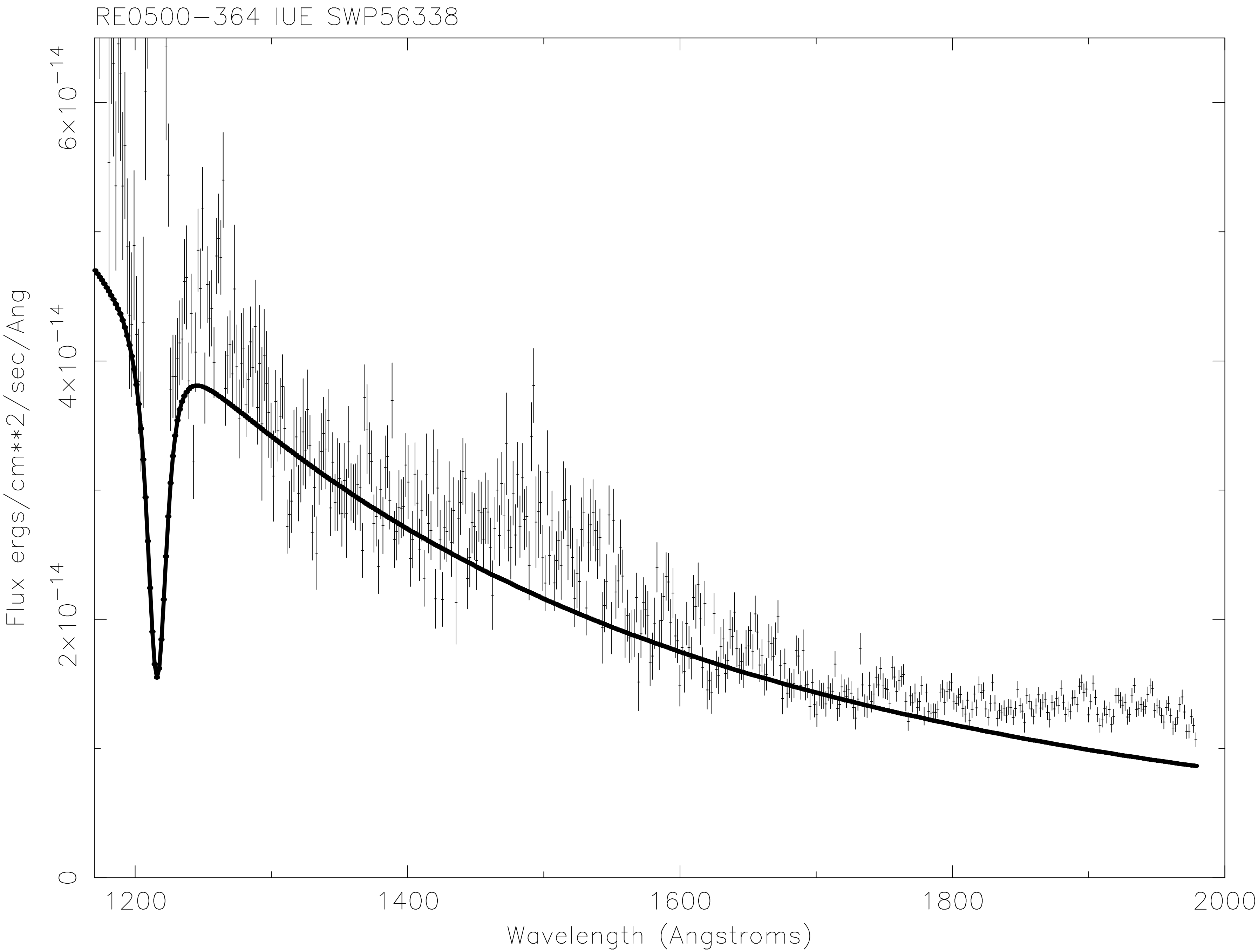

RE0500−364 IUE SWP56338
Flux ergs/cm**2/sec/Ang
6×10⁻¹⁴
4×10⁻¹⁴
2×10⁻¹⁴
0
1200
1400
1600
1800
2000
Wavelength (Angstroms)

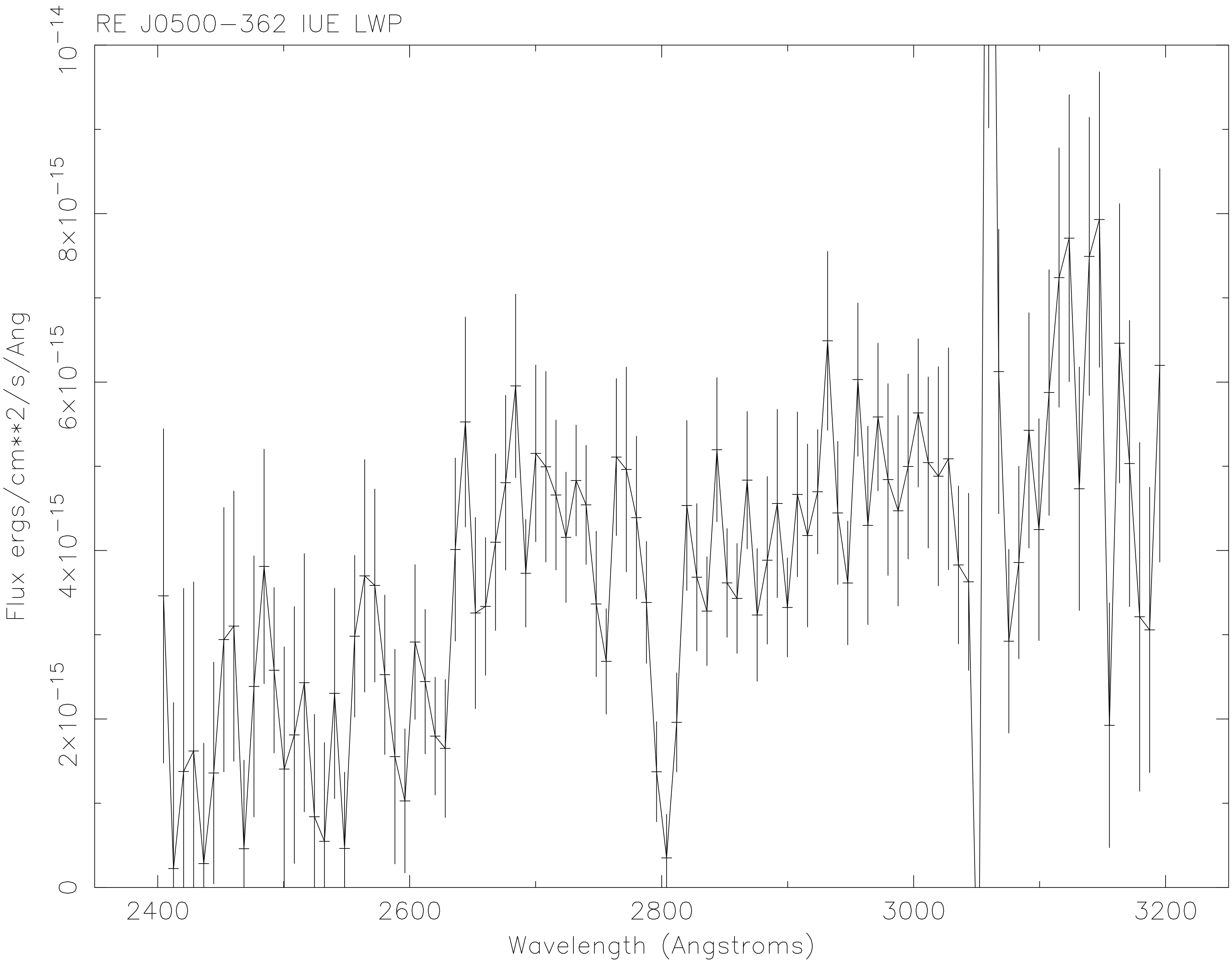
RE J0500-362 IUE LWP
Flux ergs/cm**2/s/Ang
0
2×10^{-15}
4×10^{-15}
6×10^{-15}
8×10^{-15}
10^{-14}
2400
2600
2800
3000
3200
Wavelength (Angstroms)

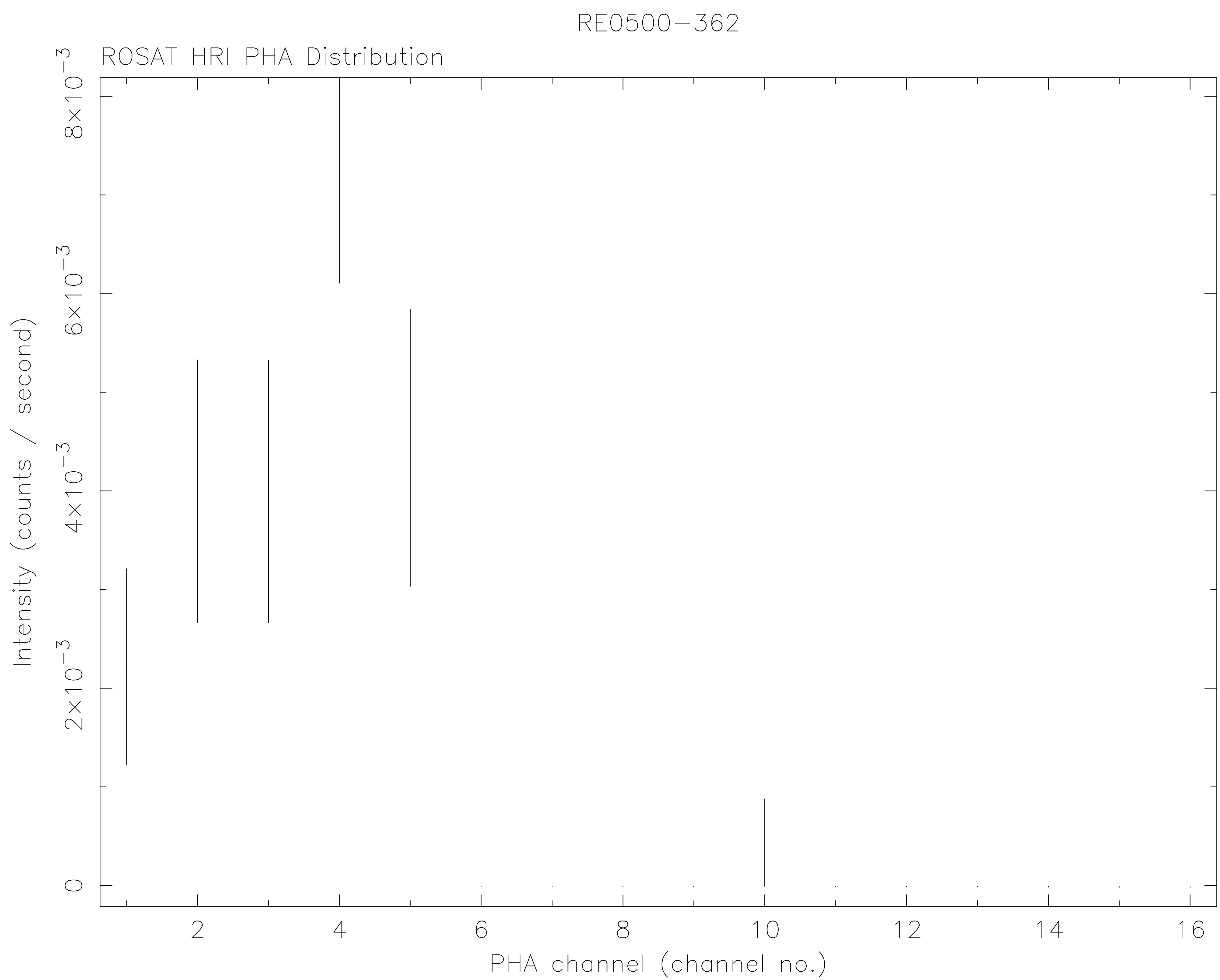
RE0500-362
ROSAT HRI PHA Distribution
Intensity (counts / second)
8×10^-3
6×10^-3
4×10^-3
2×10^-3
0
2
4
6
8
10
12
14
16
PHA channel (channel no.)

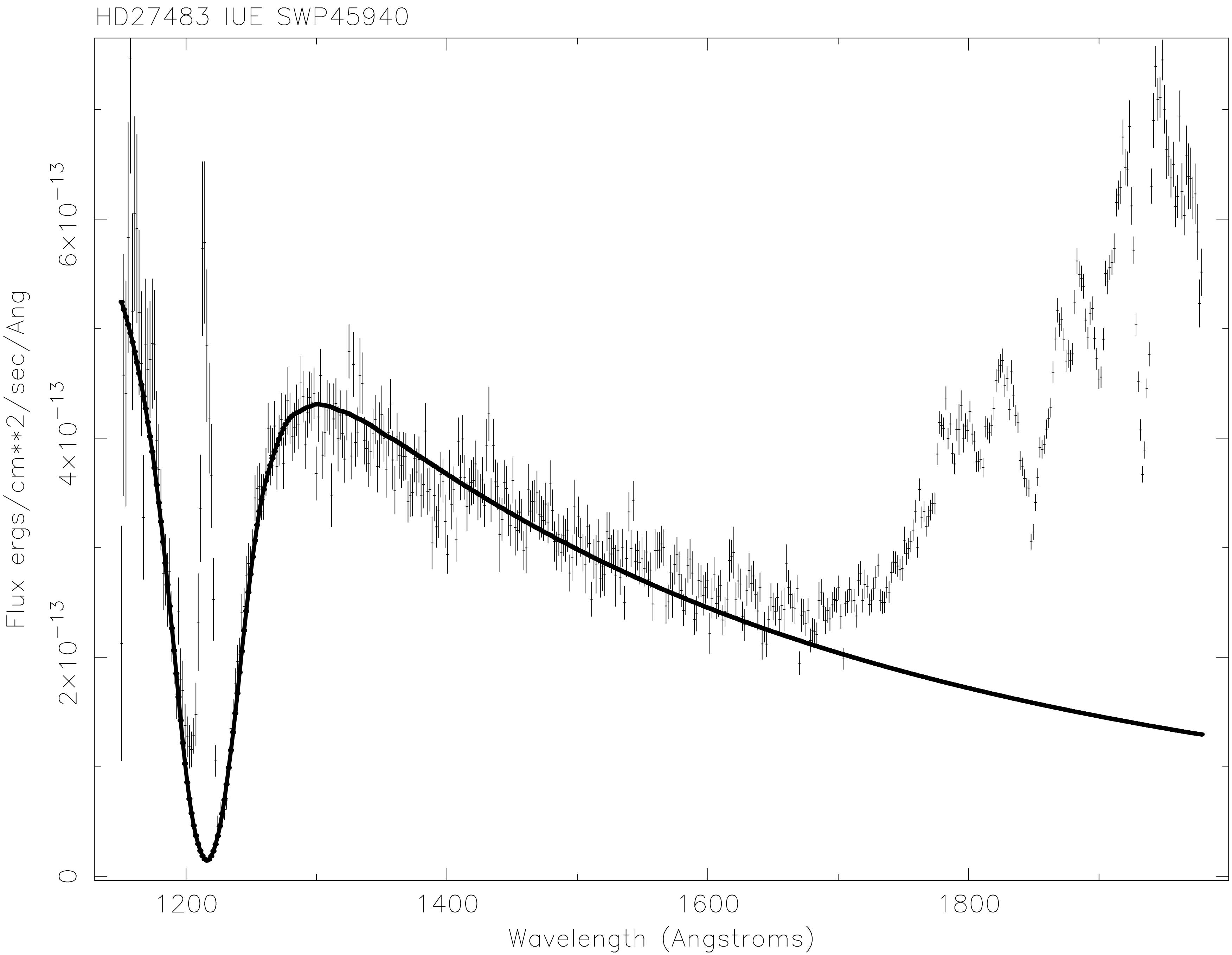
HD27483 IUE SWP45940
Flux ergs/cm**2/sec/Ang
0
2×10⁻¹³
4×10⁻¹³
6×10⁻¹³
1200
1400
1600
1800
Wavelength (Angstroms)

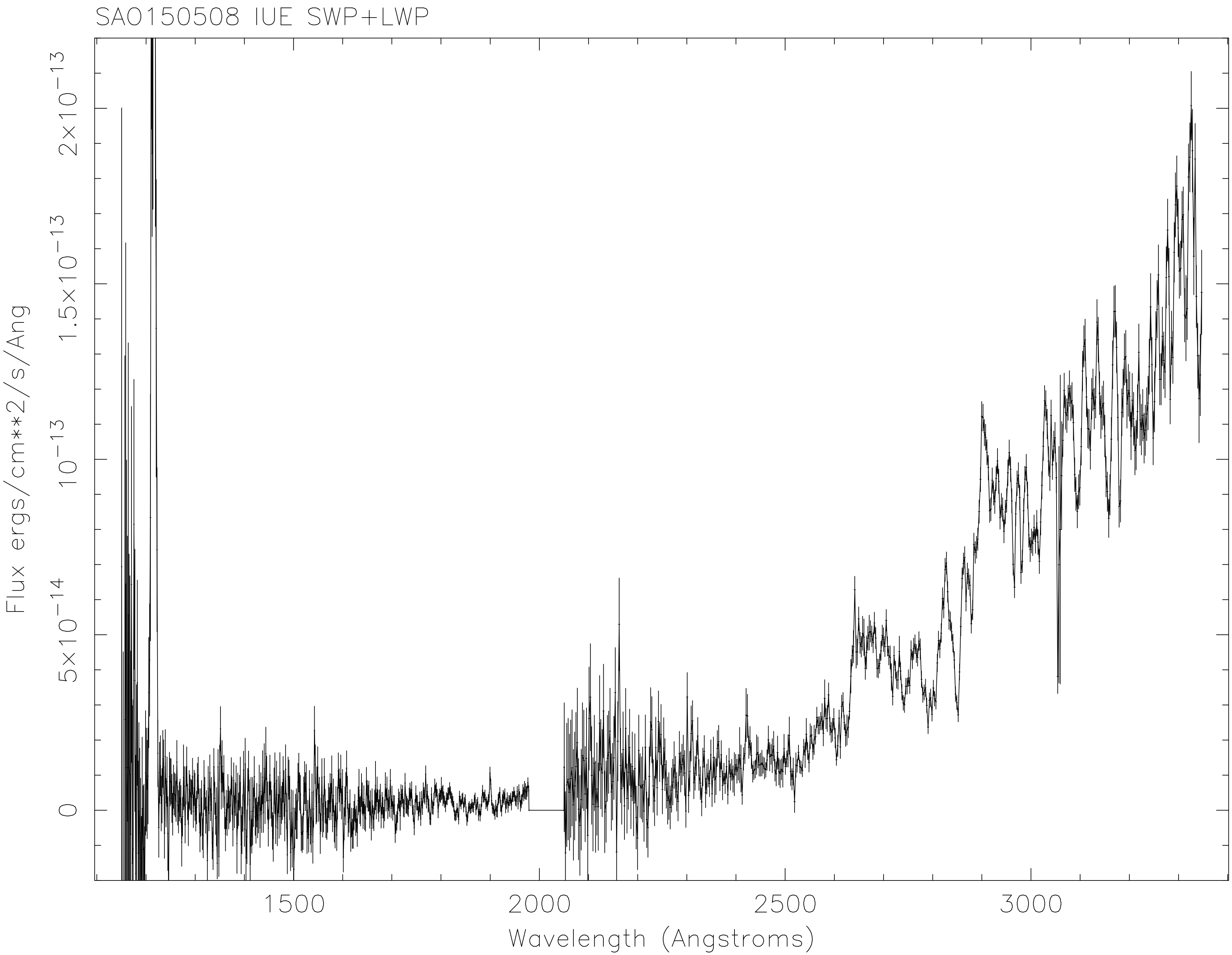

SAO150508 IUE SWP+LWP
Flux ergs/cm**2/s/Ang
0
5×10^{-14}
10^{-13}
1.5×10^{-13}
2×10^{-13}
1500
2000
2500
3000
Wavelength (Angstroms)

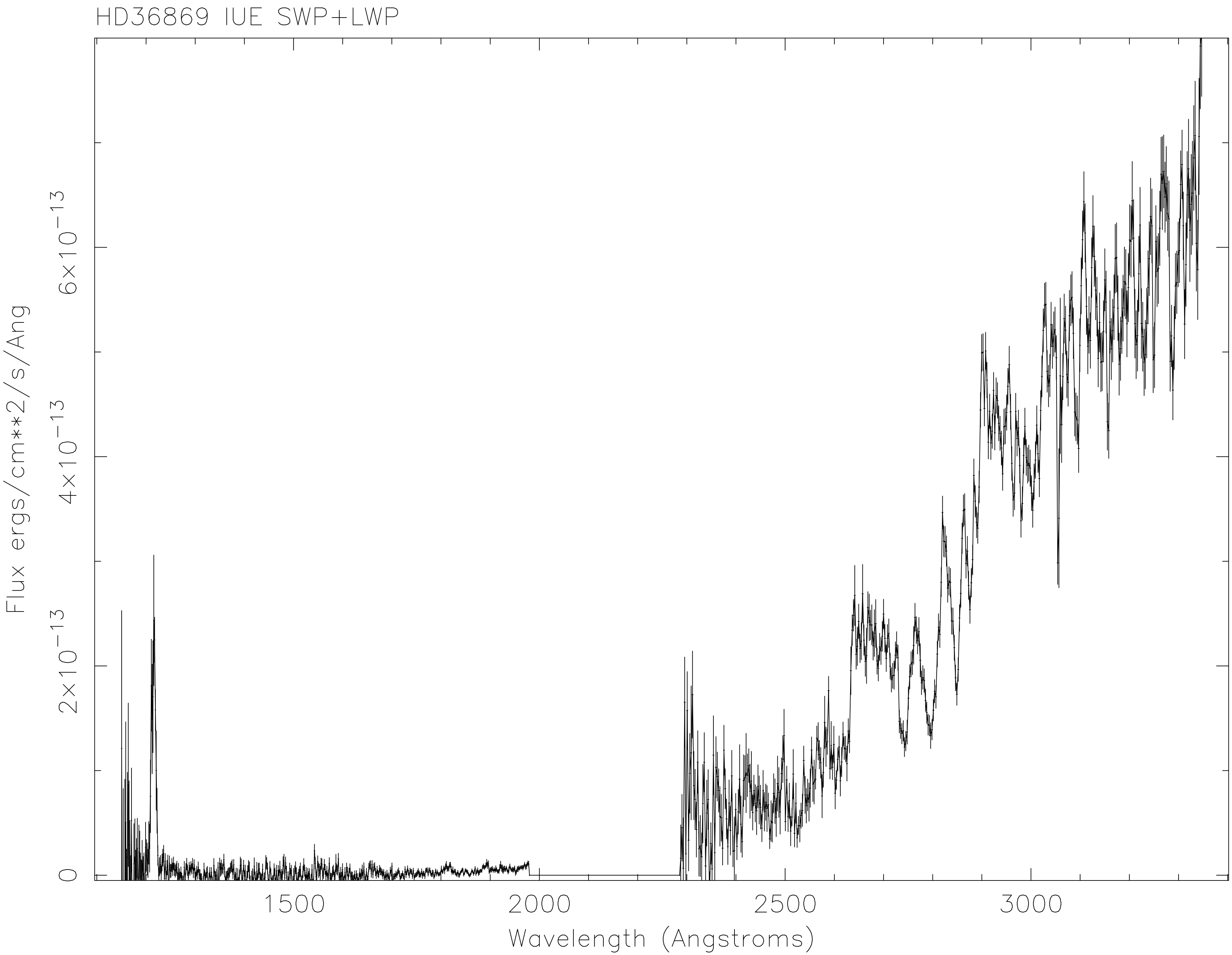

HD36869 IUE SWP+LWP
Flux ergs/cm**2/s/Ang
0
2×10−13
4×10−13
6×10−13
1500
2000
2500
3000
Wavelength (Angstroms)

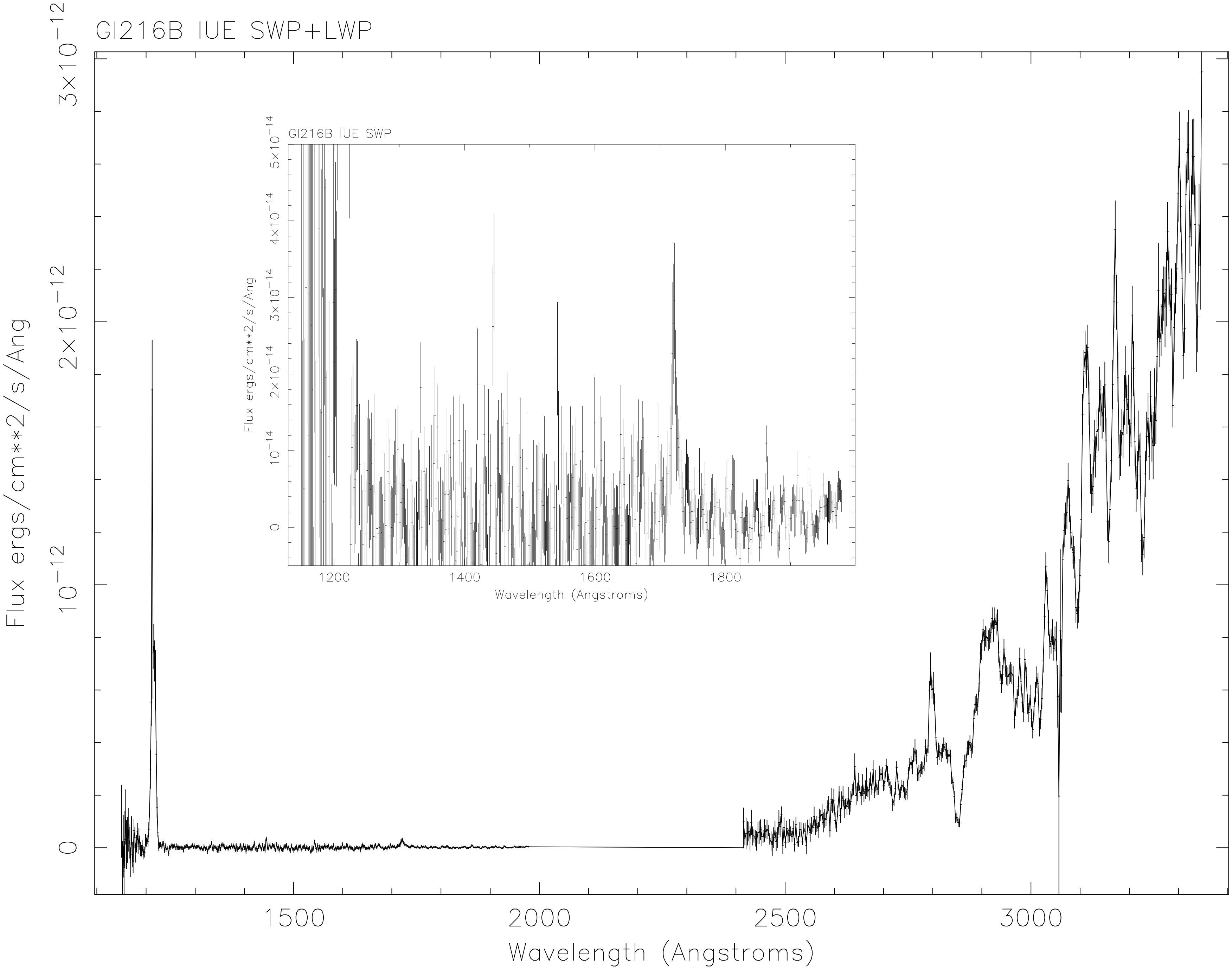
GI216B IUE SWP+LWP
Flux ergs/cm**2/s/Ang
3×10^{-12}
2×10^{-12}
10^{-12}
0
1500
2000
2500
3000
Wavelength (Angstroms)
GI216B IUE SWP
5×10^{-14}
4×10^{-14}
3×10^{-14}
2×10^{-14}
10^{-14}
1200
1400
1600
1800

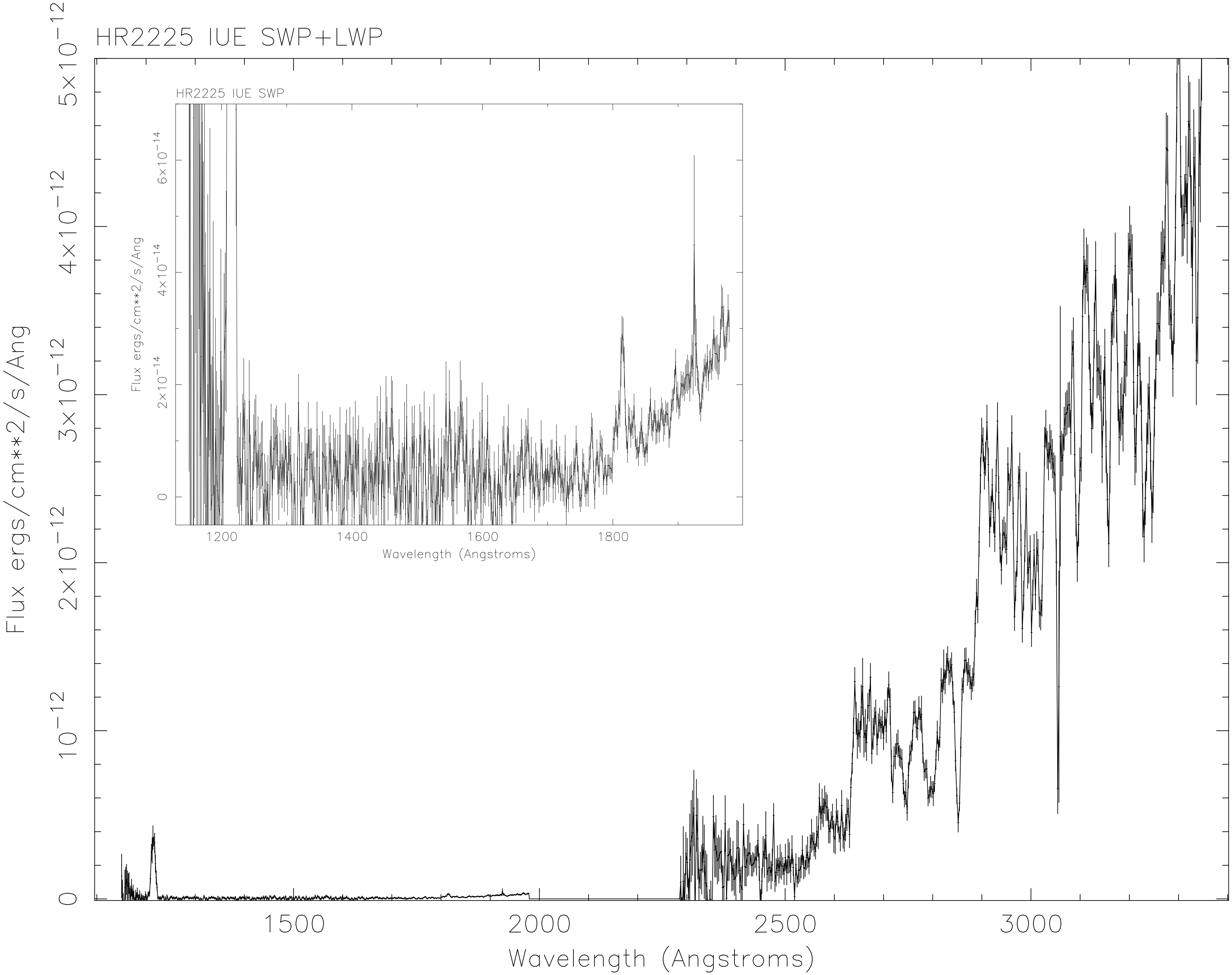
HR2225 IUE SWP+LWP
Flux ergs/cm**2/s/Ang
Wavelength (Angstroms)
0
10^{-12}
2×10^{-12}
3×10^{-12}
4×10^{-12}
5×10^{-12}
1500
2000
2500
3000
HR2225 IUE SWP
Flux ergs/cm**2/s/Ang
Wavelength (Angstroms)
0
2×10^{-14}
4×10^{-14}
6×10^{-14}
1200
1400
1600
1800

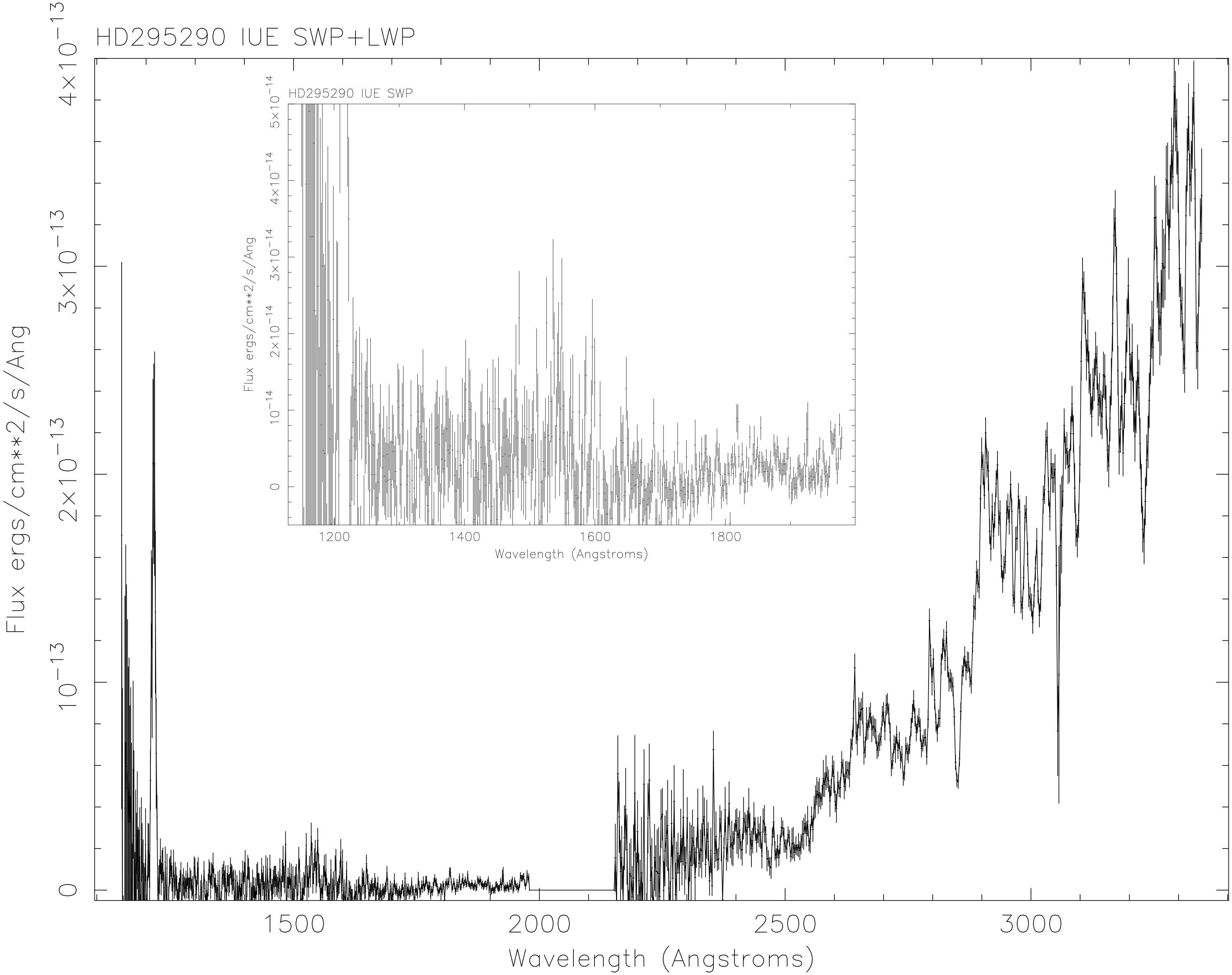

HD295290 IUE SWP+LWP
Flux ergs/cm**2/s/Ang
Wavelength (Angstroms)
0
10^{-13}
2×10^{-13}
3×10^{-13}
4×10^{-13}
1500
2000
2500
3000
HD295290 IUE SWP
10^{-14}
2×10^{-14}
3×10^{-14}
4×10^{-14}
5×10^{-14}
1200
1400
1600
1800

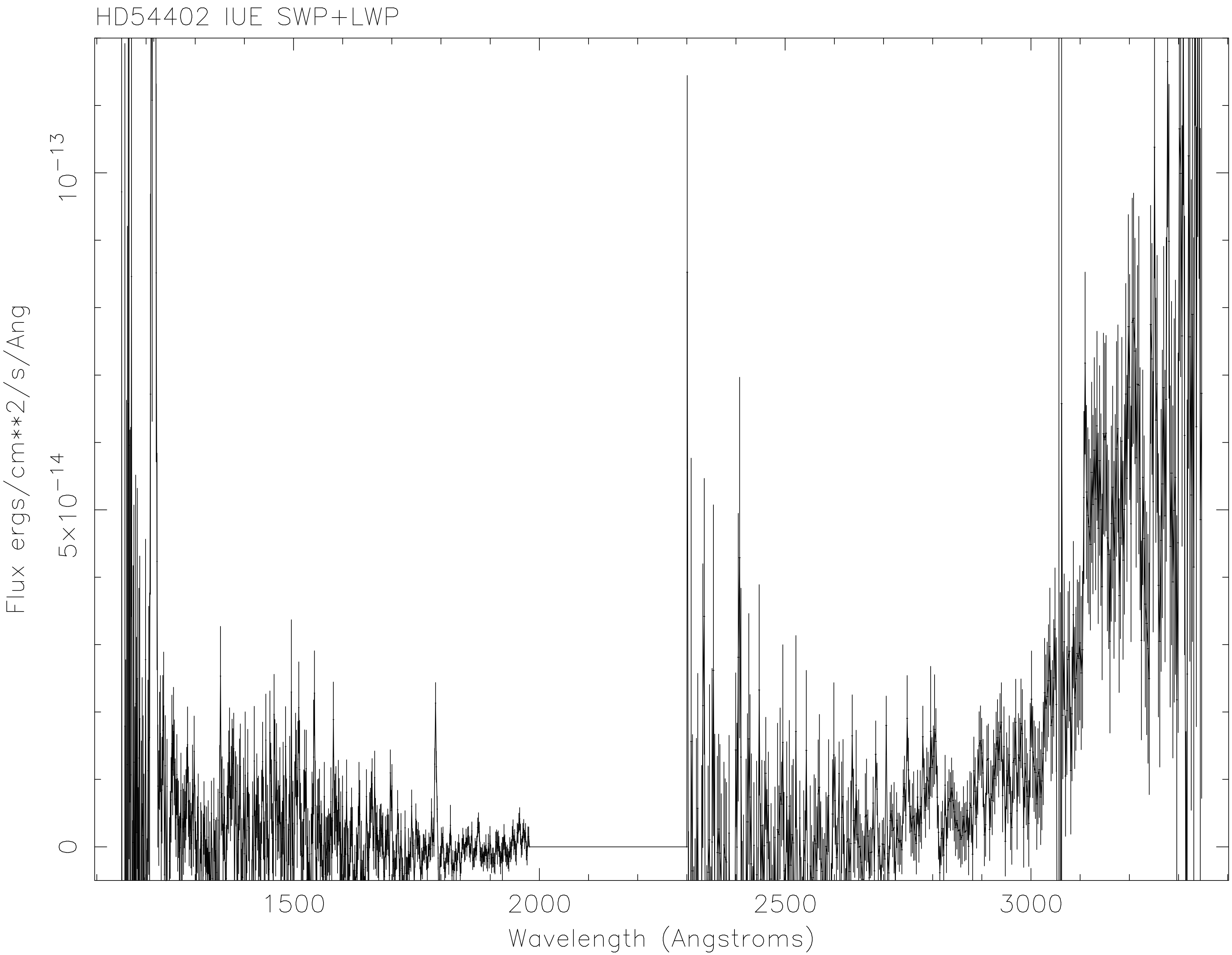

HD54402 IUE SWP+LWP
Flux ergs/cm**2/s/Ang
10^-13
5x10^-14
0
1500
2000
2500
3000
Wavelength (Angstroms)

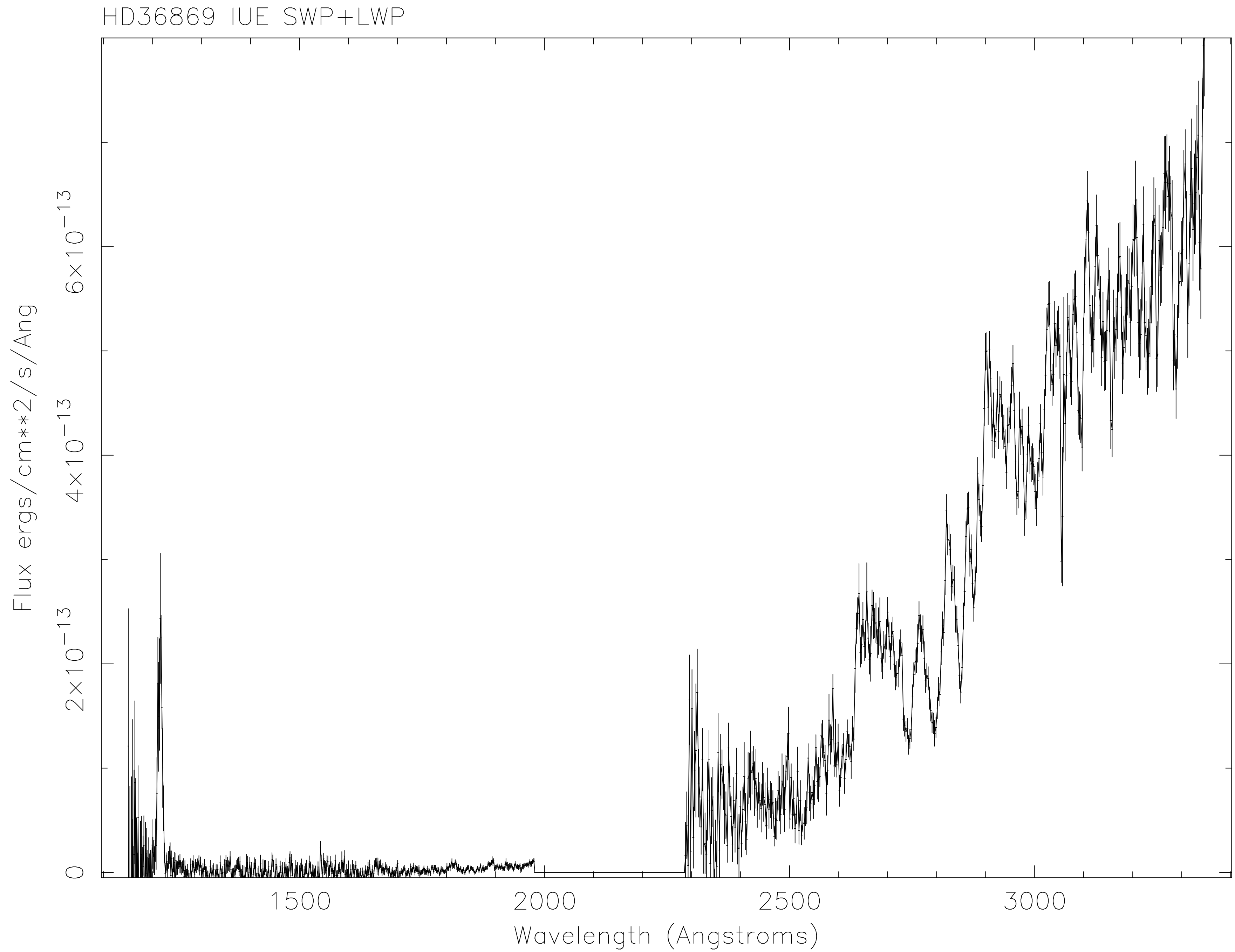
HD36869 IUE SWP+LWP
Flux ergs/cm**2/s/Ang
0
2×10⁻¹³
4×10⁻¹³
6×10⁻¹³
1500
2000
2500
3000
Wavelength (Angstroms)

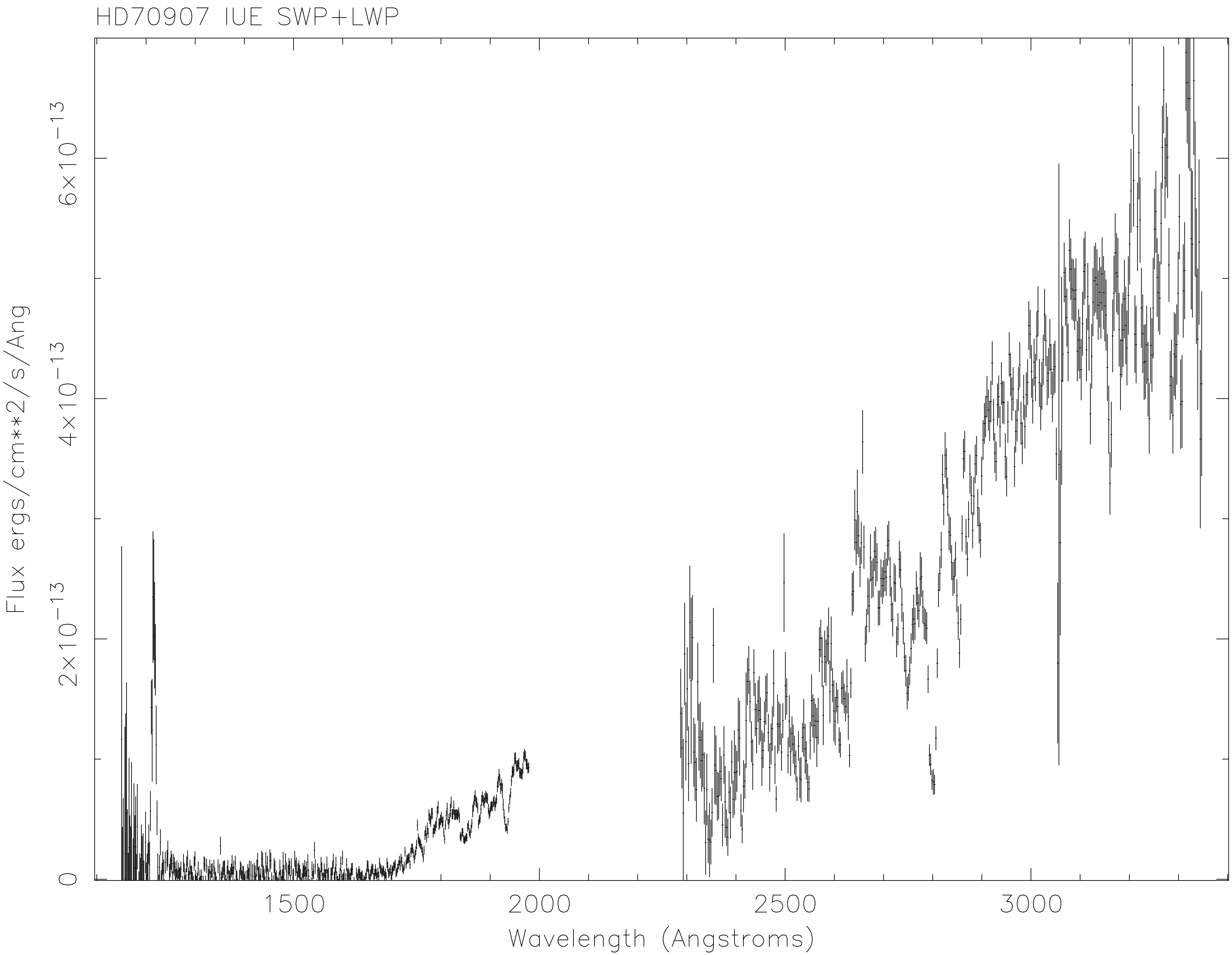
HD70907 IUE SWP+LWP
Flux ergs/cm**2/s/Ang
0
2×10⁻¹³
4×10⁻¹³
6×10⁻¹³
1500
2000
2500
3000
Wavelength (Angstroms)

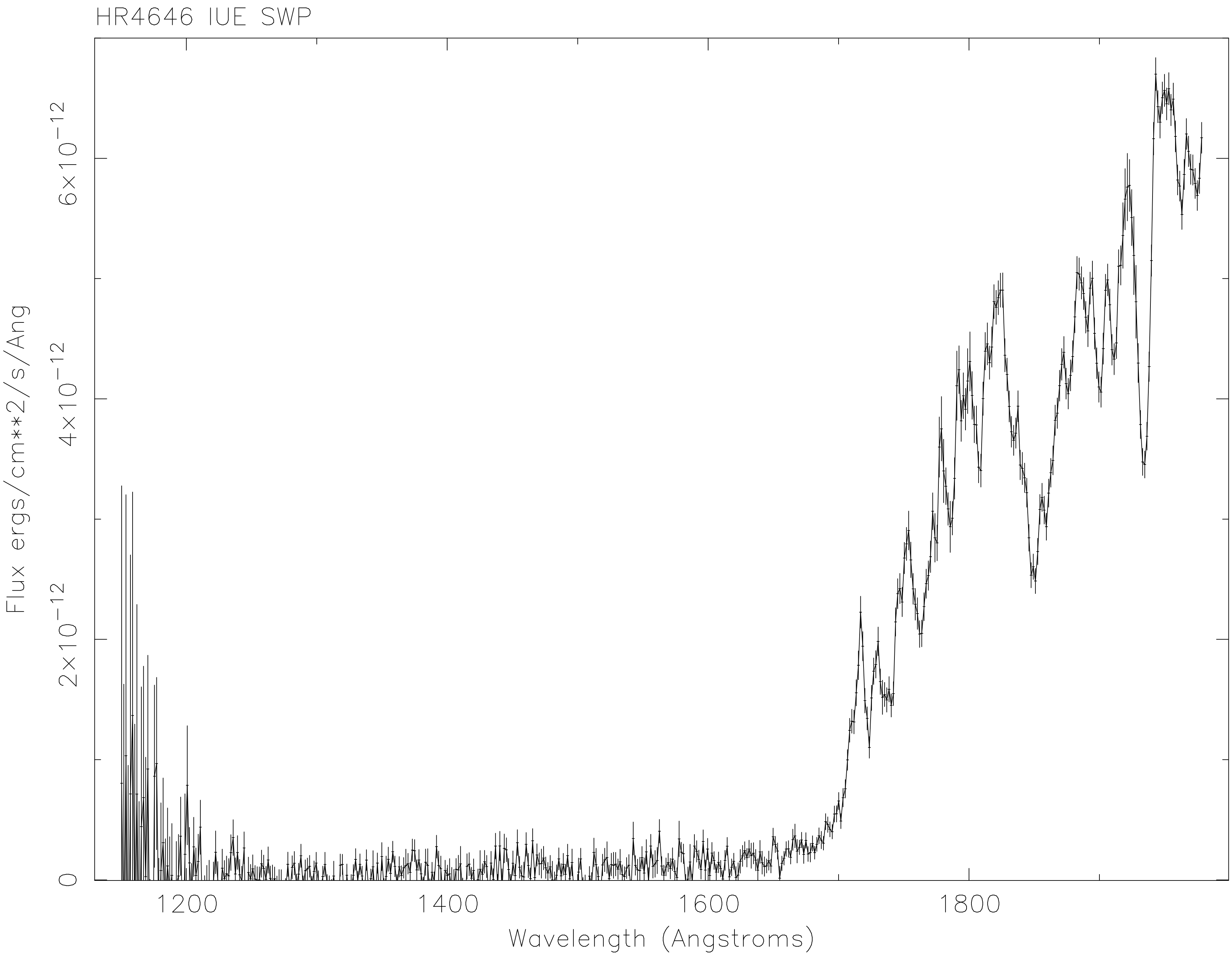

HR4646 IUE SWP
Flux ergs/cm**2/s/Ang
0
2×10⁻¹²
4×10⁻¹²
6×10⁻¹²
1200
1400
1600
1800
Wavelength (Angstroms)